

# Vortex lattice structure in a $d_{x^2-y^2}$ -wave superconductor

Masanori Ichioka, Naoki Enomoto, and Kazushige Machida  
*Department of Physics, Okayama University, Okayama 700, Japan*  
(May 15, 2019)

The vortex lattice structure in a  $d_{x^2-y^2}$ -wave superconductor is investigated near the upper critical magnetic field in the framework of the Ginzburg Landau theory extended by including the correction terms such as the higher order derivatives derived from the Gor'kov equation. On lowering temperature, the unit cell shape of the vortex lattice gradually varies from a regular triangular lattice to a square lattice through the shape of an isosceles triangle. As for the orientation of the vortex lattice, the base of an isosceles triangle is along the  $a$  axis or the  $b$  axis of the crystal. The fourfold symmetric structure around a vortex core is also studied in the vortex lattice case. It is noted that these characteristic features appear even in the case the induced  $s$ -wave order parameter is absent around the vortex of the  $d_{x^2-y^2}$ -wave superconductivity. We also investigate the effect of the induced  $s$ -wave order parameter. It enhances (suppresses) these characteristic features of the  $d_{x^2-y^2}$ -wave superconductor when the  $s$ -wave component of the interaction is attractive (repulsive).

PACS numbers: 74.72.-h, 74.60.-w, 74.60.Ec, 74.20.De

## I. INTRODUCTION

Much attention has been focused on a vortex structure in a high- $T_c$  superconductor. It is of great interest how the vortex structure of the high- $T_c$  superconductor is different from that of a conventional superconductor. Various investigations of the flux line lattice (or vortex lattice) for conventional superconductors are compiled in Ref. 1, including the gap and Fermi surface anisotropy effects. By a number of experimental and theoretical investigations, it is concluded that the symmetry of this superconductor is most likely to be  $d_{x^2-y^2}$ -wave. Therefore, one of the points is how the vortex structure of a  $d_{x^2-y^2}$ -wave superconductor is different from that of an isotropic  $s$ -wave superconductor. The amplitude of the  $d_{x^2-y^2}$ -wave pairing, i.e.,  $\hat{k}_x^2 - \hat{k}_y^2$  in momentum space, has fourfold symmetry for the rotation about the  $c$ -axis. We expect that, reflecting this symmetry, the core structure of an isolated single vortex may break the cylindrical symmetry and show fourfold symmetry in a  $d_{x^2-y^2}$ -wave superconductor, and the fourfold symmetry of the core structure may affect the vortex lattice structure.

Keimer *et al.*<sup>2</sup> observed an oblique lattice by a small-angle neutron scattering (SANS) study of the vortex lattice in  $\text{YBa}_2\text{Cu}_3\text{O}_7$  in a magnetic field region of  $0.5\text{T} \leq H \leq 5\text{T}$  applied parallel to the  $c$  axis. They reported that the vortex lattice has an angle of  $73^\circ$  between the two primitive vectors and is oriented such that the nearest-neighbor direction of vortices makes an angle of  $45^\circ$  with the  $a$  axis. The oblique lattice with  $77^\circ$  was also found by scanning tunneling microscopy (STM) at 6T by Maggio-Aprile *et al.*<sup>3,4</sup> They observed the elliptic-shaped STM image of the vortex core, and concluded that this oblique lattice cannot be explained by considering only the effect of the intrinsic in-plane anisotropy, that is, the difference of the coherence lengths between the  $a$  axis and the  $b$  axis directions.<sup>4,5</sup> On the other hand, at low fields of 35 and 65G, Dolan *et al.*<sup>6</sup> reported the regular triangular lattice by the Bitter-pattern observation of the vortices, where the slight distortion of the vortex lattice is explained by the anisotropy of the coherence lengths between the  $a$  axis and the  $b$  axis directions. It is suggested that this deformation from the regular triangular lattice in the high field region of a  $d_{x^2-y^2}$ -wave superconductor is due to the effect of the fourfold symmetric vortex core structure.

The fourfold symmetric vortex core structure in a  $d_{x^2-y^2}$ -wave superconductor was so far derived theoretically when the  $s$ -wave component is induced around a vortex of  $d_{x^2-y^2}$ -wave superconductivity.<sup>7-14</sup> This mixing scenario was mainly put forth by Berlinsky *et al.*<sup>7,8</sup> and Ren *et al.*<sup>10-12</sup> in the two-component Ginzburg Landau (GL) theory for  $s$ - and  $d$ -wave superconductivity. According to the consideration based on the two-component GL theory, it is possible that the  $s$ -wave component is coupled with the  $d$ -wave component through the gradient terms. Therefore, the  $s$ -wave component may be induced when the  $d$ -wave order parameter spatially varies, such as near the vortex or interface under certain restricted conditions.<sup>11,15</sup> The induced  $s$ -wave component around the vortex is fourfold symmetric. The resulting vortex structure in the  $d$ -wave superconductor, therefore, exhibits fourfold symmetry.

However, it is noted that the amplitude of the induced  $s$ -wave order parameter strongly depends on the detail of the pairing interaction. In the weak coupling theory of the continuum model, for example, we define that the  $s$ -wave component of the order parameter is proportional to  $V_s$ , the  $s$ -wave component of the pairing interaction.<sup>14</sup> Therefore, when  $|V_s|$  is negligibly small compared with the dominant  $d_{x^2-y^2}$ -wave component of the pairing interaction,

the induced  $s$ -wave order parameter can be neglected. On the other hand, it was reported that in the Bogoliubov-de Gennes theory of the extended Hubbard model the amplitude of the induced  $s$ -wave order parameter is suppressed when the on-site repulsion of the interaction increases.<sup>13</sup> In the numerical calculation by Wang and MacDonald,<sup>16</sup> the induced  $s$ -wave order parameter is small, on the order of a few percents of the dominant  $d_{x^2-y^2}$ -wave component.

For a moment, we consider the limit where the induced  $s$ -wave order parameter is negligibly small compared with the dominant  $d_{x^2-y^2}$ -wave component. (We denote this limit as “pure  $d_{x^2-y^2}$ -wave”.) In this case, the two-component GL equations are reduced to a one-component GL equation for only a  $d_{x^2-y^2}$ -wave component, which is the same form as that of the isotropic  $s$ -wave case within the conventional GL theory. Thus, the conventional GL theory gives the result that the vortex structure in a pure  $d_{x^2-y^2}$ -wave superconductor is exactly the same as that of an isotropic  $s$ -wave one, that is, the core structure of a single vortex is circular symmetric and the vortex lattice is the triangular Abrikosov lattice structure.<sup>17</sup>

However, Ichioka *et al.*<sup>18</sup> showed that the core structure of a single vortex exhibits the fourfold symmetric structure even in a pure  $d_{x^2-y^2}$ -wave superconductor by a numerical calculation based on the quasi-classical Eilenberger theory, which can be applied even at low temperatures. In their calculation, the fourfold symmetric structure becomes clear on lowering temperature  $T$ . These facts indicate the following results. Strictly speaking, the conventional GL equation is valid only near the transition temperature  $T_c$ . Far from  $T_c$ , we have to include several correction terms which is higher order in the small parameter  $\ln(T_c/T) \simeq 1 - T_c/T$ . Enomoto *et al.*<sup>19</sup> showed that the correction terms consist of higher order terms of the order parameter and the higher derivatives (or non-local terms) which are neglected in the conventional GL theory. And they indeed succeeded in showing that the fourfold symmetric core structure of a single vortex in a pure  $d_{x^2-y^2}$ -wave superconductor is reproduced by including these correction terms. This indicates that, in the study of the fourfold symmetric vortex core structure in a  $d_{x^2-y^2}$ -wave superconductor, we have to consider the effect of the correction terms of the order  $\ln(T_c/T)$  in addition to the effect of the induced  $s$ -wave order parameter. These correction terms may affect the structure of the vortex lattice.

As for the effect of the induced  $s$ -wave order parameter on the vortex lattice structure, Berlinsky *et al.*<sup>7-9</sup> investigated it by using the two-component GL equations. As characteristic features of the  $d_{x^2-y^2}$ -wave superconductor’s vortex lattice, they suggested that the vortex lattice is deformed from a triangular lattice due to the induced  $s$ -wave order parameter and it leads to the double peak structure in the magnetic field distribution function  $P(h)$  as a function of magnetic field  $h$ . In a pure  $d_{x^2-y^2}$ -wave superconductor, however, these features vanish within their theory since the induced  $s$ -wave order parameter is absent. On the other hand, the correction terms which introduce the fourfold symmetric core structure might give some effects on the vortex lattice structure even in the pure  $d_{x^2-y^2}$ -wave superconductor. In the study of the vortex lattice based on the GL framework, the effect of the correction terms in a  $d_{x^2-y^2}$ -wave superconductor has not been studied sufficiently.

The purpose of this paper is to determine the orientation and the unit cell shape of the vortex lattice in the framework of the extended GL theory near the upper critical magnetic field  $H_{c2}$ . We also investigate the spatial variation of the vortex lattice structure, that is, the order parameter, the current and the induced magnetic field. In addition to the effect of the correction terms of the  $d_{x^2-y^2}$ -wave superconductivity in the order  $\ln(T_c/T)$ , our calculation is performed by including also the effect of the induced  $s$ -wave component so that the contribution of both effects (the effects of the correction terms and of the induced  $s$ -wave component) can be estimated on the equal footing. Therefore, we reconstruct the two-component GL theory for  $s$ - and  $d_{x^2-y^2}$ -wave order parameters with including the correction terms of the order  $\ln(T_c/T)$ . The pure  $d_{x^2-y^2}$ -wave case is easily obtained in the limit where the amplitude of the  $s$ -wave order parameter is negligibly small.

We consider the case of the vortex lattice under a magnetic field applied parallel to the  $c$  axis (or  $z$  axis) in the clean limit. Our consideration is restricted in the case of tetragonal symmetry described by the point group  $D_4$ . Then, the  $a$  axis and the  $b$  axis of the crystal coordinate are equivalent each other. The orthorhombic symmetry case can be obtained by scaling the coordinate system, namely, the  $a$  axis direction and the  $b$  axis direction are made to be equivalent if the lengths are scaled by the coherence length of each direction. The Fermi surface is assumed to be two-dimensional, which is appropriate to high- $T_c$  superconductors, and isotropic in order to clarify effects of the  $d_{x^2-y^2}$ -wave nature of the pair potential on the vortex lattice structure. The additional anisotropy coming from, e.g., the Fermi surface can be incorporated into our extended GL framework.

The two-component GL equations were derived, for example, by Ren *et al.*<sup>11,12</sup> from the Gor’kov equation. However, their derivation is within the conventional GL framework. Here, to study the effect of correction terms of the order  $\ln(T_c/T)$ , we reconstruct the GL theory by including higher order terms of the order parameter and the higher derivatives other than terms in the conventional GL theory. In the pure  $d_{x^2-y^2}$ -wave case, the present authors derived the GL equation with including these correction terms from the Gor’kov equation for the continuum model to study the fourfold symmetric core structure of a single vortex.<sup>19</sup> In this paper, we derive the two-component GL equation for  $s$ - and  $d_{x^2-y^2}$ -wave components from the Gor’kov equation with including the correction terms of the order  $\ln(T_c/T)$ . For simplicity of calculation, our derivation is performed in the weak coupling theory of the continuum model. As for other models, for example, Feder and Kallin derived the two-component GL equations from the extended Hubbard

model with including these higher order terms.<sup>20</sup> In the GL equation derived from other model, the coefficient of each term is modified, but the derived terms have one-to-one correspondence to those of ours. Therefore, while our results may be modified quantitatively, our approach can be applied to the GL equation derived from other models and our results remain to be valid qualitatively.

We calculate the  $d_{x^2-y^2}$ -wave and the induced  $s$ -wave components of the order parameter near  $H_{c2}$  by solving the linearized version of the derived GL equations. We also calculate the current and the induced magnetic field in the vortex lattice near  $H_{c2}$  by using the current density expression which includes the contribution of the correction terms and the induced  $s$ -wave order parameter. In our calculation of the vortex lattice structure, we use the magnetic Bloch state (or Eilenberger's basis function)<sup>21</sup> as the basis function and expand various quantities in powers of  $\ln(T_c/T)$ . Then, we can determine the vortex lattice structure in terms of an analytically expressed form, which makes it easy to understand the detail of the properties of the vortex lattice, such as the dependence on the mixing of the  $s$ -wave component.

As for the orientation and the unit cell shape of the vortex lattice, the equilibrium state is estimated by the minimum of the free energy. This was done by Abrikosov near  $H_{c2}$  within the conventional GL theory for an isotropic  $s$ -wave superconductor.<sup>17</sup> Here, we have to extend his theory so that we can include the effects of the correction terms and of the induced  $s$ -wave order parameter. The extension about the effect of the induced  $s$ -wave order parameter was done by Berlinsky *et al.*<sup>7,8</sup> The extension about the effect of the correction terms was performed by Takanaka in the case of isotropic  $s$ -wave pairing but anisotropic density of states at the Fermi surface.<sup>22</sup> In this paper, we follow the method provided by Takanaka and extend his calculation to the case where the superconductivity is  $d_{x^2-y^2}$ -wave symmetry and the induced  $s$ -wave order parameter also exists.

On the other hand, Won and Maki<sup>23,24</sup> studied the vortex lattice structure near  $H_{c2}$  numerically from the Gor'kov equation on the same stand point of ours. They suggested that the most stable configuration of the vortex lattice is a square lattice tilted by  $\pi/4$  from the  $a$  axis at temperature  $T \leq 0.88T_c$  even in the pure  $d_{x^2-y^2}$ -wave case. In our interpretation, this deformation of the vortex lattice from a triangular lattice is due to the above-mentioned correction terms of the order  $\ln(T_c/T)$ , which are derived from the Gor'kov equation but neglected in the conventional GL theory. Our calculation is based on the GL expansion of the Gor'kov equation. Therefore, their numerical results are reproduced near  $T_c$  by our calculation as an analytically expressed form. We note that Won and Maki made some errors in their estimate of the free energy minimum. They estimated the free energy minimum by the Abrikosov parameter  $\beta_A$  which is originally used within the conventional GL theory. However, this expression of  $\beta_A$  itself should be modified by including the correction of the order  $\ln(T_c/T)$ . In their calculation, the free energy is estimated only in the case of a regular triangular lattice and a square lattice. In addition to them, the oblique lattice should be considered together. In our calculation, we derive the correct expression of the Abrikosov parameter. And, by using it, we estimate the free energy minimum by exhausting all the possible orientation and unit cell shape of the vortex lattice structure, including a shape of a scalene triangle.

The rest of this paper is organized as follows. In Sec. II, we construct the two-component GL equations with including the correction terms of the order  $\ln(T_c/T)$ . By using these equations, the  $d_{x^2-y^2}$ -wave and the induced  $s$ -wave component of the order parameter are calculated near  $H_{c2}$ . In Sec. III, we calculate the current and the induced magnetic field in the vortex lattice state near  $H_{c2}$ . The orientation and the unit cell shape of the equilibrium vortex lattice structure is determined by the free energy minimum in Sec. IV. In Sec. V, we present the spatial variation of the vortex lattice structure in the pure  $d_{x^2-y^2}$ -wave case. The summary and discussions are given in Sec. VI.

## II. ORDER PARAMETER NEAR $H_{c2}$

We adopt the coordinate system shown in Fig. 1, where one of the unit vectors of the vortex lattice is along the  $x$  axis. Thus, the unit vectors of the vortex lattice are given by  $\mathbf{r}_1 = (a_x, 0)$  and  $\mathbf{r}_2 = (\zeta a_x, a_y)$ . The  $x$  axis forms an angle of  $\theta_0$  from the  $a$  axis of the crystal coordinate as shown in Fig. 1. Therefore the shape of the vortex lattice is characterized by  $a_y/a_x$  and  $\zeta$ , and the orientation of the vortex lattice is denoted by  $\theta_0$ .

We consider the two-component GL theory for  $s$ - and  $d_{x^2-y^2}$ -wave superconductivity. The order parameter (or pair potential) is given by

$$\Delta(\mathbf{r}, \theta) = s(\mathbf{r})\phi_s(\theta) + d(\mathbf{r})\phi_d(\theta). \quad (2.1)$$

Here,  $\mathbf{r} = (x, y)$  is the center of mass coordinate of the Cooper pair. The direction of relative momentum of the Cooper pair is denoted by an angle  $\theta$  measured from the  $x$  axis in the  $ab$  plane. The symmetry function for  $s$ -wave ( $d_{x^2-y^2}$ -wave) component  $\phi_s(\theta)$  ( $\phi_d(\theta)$ ) is assumed to be real and to satisfy the normalization condition  $\langle \phi_s^2 \rangle = 1$  ( $\langle \phi_d^2 \rangle = 1$ ). Here, we write  $\int (\dots) d\theta / 2\pi = \langle \dots \rangle$ . In our presentation of figures, we use forms

$$\phi_s(\theta) = 1, \quad \phi_d(\theta) = \sqrt{2} \cos 2(\theta - \theta_0) \quad (2.2)$$

as an example. On the other hand, the pairing interaction is assumed to be separable as follows,

$$V(\theta', \theta) = V_s \phi_s(\theta') \phi_s(\theta) + V_d \phi_d(\theta') \phi_d(\theta), \quad (2.3)$$

where attractive interaction is treated as positive. In Eq. (2.3), the  $d_{x^2-y^2}$ -wave component  $V_d$  is dominant and the  $s$ -wave component  $V_s$  is smaller than  $V_d$ .

The GL equation is derived as follows from the Gor'kov equation in the weak coupling theory of the continuum model (As for the detail of the derivation, see Appendix A of Ref. 19. Now,  $\eta(\mathbf{r})\phi(\mathbf{k})$  and  $\bar{V}\phi^*(\mathbf{k})\phi(\mathbf{k}')$  are denoted by  $\Delta(\mathbf{r}, \theta)$  and  $V(\theta, \theta')$ , respectively.),

$$\begin{aligned} N_F^{-1} \Delta(\mathbf{r}, \theta') &= A_0 \langle V(\theta', \theta) \Delta(\mathbf{r}, \theta) \rangle + A_2 v_F^2 \langle V(\theta', \theta) (\hat{\mathbf{v}} \cdot \mathbf{q})^2 \Delta(\mathbf{r}, \theta) \rangle + A_2 \langle V(\theta', \theta) |\Delta(\mathbf{r}, \theta)|^2 \Delta(\mathbf{r}, \theta) \rangle \\ &+ A_4 v_F^4 \langle V(\theta', \theta) (\hat{\mathbf{v}} \cdot \mathbf{q})^4 \Delta(\mathbf{r}, \theta) \rangle + 6A_4 \langle V(\theta', \theta) |\Delta(\mathbf{r}, \theta)|^4 \Delta(\mathbf{r}, \theta) \rangle \\ &+ 2A_4 v_F^2 \langle V(\theta', \theta) [4\{(\hat{\mathbf{v}} \cdot \mathbf{q})^2 \Delta(\mathbf{r}, \theta)\} |\Delta(\mathbf{r}, \theta)|^2 + \Delta(\mathbf{r}, \theta)^2 \{(\hat{\mathbf{v}} \cdot \mathbf{q})^2 \Delta(\mathbf{r}, \theta)\}^* \\ &- 2|(\hat{\mathbf{v}} \cdot \mathbf{q}) \Delta(\mathbf{r}, \theta)|^2 \Delta(\mathbf{r}, \theta) + 3\{(\hat{\mathbf{v}} \cdot \mathbf{q}) \Delta(\mathbf{r}, \theta)\}^2 \Delta^*(\mathbf{r}, \theta)] \rangle + (\text{higher order terms}) \end{aligned} \quad (2.4)$$

with  $\hat{\mathbf{v}} \equiv \mathbf{v}(\theta)/v_F = (\cos \theta, \sin \theta)$  and  $\mathbf{q} = \nabla/i + (2\pi/\phi_0)\mathbf{A}$ , where  $N_F$  is the density of states at the Fermi surface,  $v_F$  the Fermi velocity and  $\phi_0$  the flux quantum. The vector potential is given by  $\mathbf{A} = (-H_0 y, 0, 0)$  in the Landau gauge. When we consider the GL equation, the contribution of the internal magnetic field can be neglected in  $\mathbf{A}$  compared with that of the external field  $H_0$ , since we consider the case of an extreme type II superconductor. In Eq. (2.4),  $A_0 = \ln(2\omega_D \bar{\gamma}/\pi T)$  with the Debye frequency  $\omega_D$  and the Euler constant  $\bar{\gamma}$ ,  $A_2 = -\beta/3$  and  $A_4 = \alpha\beta^2/18$ , where

$$\alpha = \frac{62\zeta(5)}{49\zeta(3)^2} = 0.908\dots, \quad \beta = \frac{21\zeta(3)}{16\pi^2 T^2} \quad (2.5)$$

with Riemann's  $\zeta$ -functions  $\zeta(3)$  and  $\zeta(5)$ . The terms with  $A_4$  in Eq. (2.4) are the correction terms which are neglected within the conventional GL theory.

Substituting Eqs. (2.1) and (2.3) into Eq. (2.4) and using the relation  $(N_F V_d)^{-1} = \ln(2\omega_D \bar{\gamma}/\pi T_c)$ , we obtain two-component GL equations for  $s$ - and  $d_{x^2-y^2}$ -wave components,

$$\frac{1}{\eta_0} s + \gamma c_s \frac{2\xi^2}{\eta_0} \{ \langle \phi_s^2 (\hat{\mathbf{v}} \cdot \mathbf{q})^2 \rangle_s + \langle \phi_s \phi_d (\hat{\mathbf{v}} \cdot \mathbf{q})^2 \rangle_d \} + \gamma c_s \frac{2}{3\eta_0^3} \{ \langle \phi_s^4 \rangle |s|^2 s + \langle \phi_s^2 \phi_d^2 \rangle (2|d|^2 s + d^2 s^*) \} + O(\gamma^2) = 0, \quad (2.6)$$

$$\begin{aligned} & - \frac{1}{\eta_0} d + \frac{2\xi^2}{\eta_0} \{ \langle \phi_d^2 (\hat{\mathbf{v}} \cdot \mathbf{q})^2 \rangle_d + \langle \phi_s \phi_d (\hat{\mathbf{v}} \cdot \mathbf{q})^2 \rangle_s \} + \frac{2}{3\eta_0^3} \{ \langle \phi_d^4 \rangle |d|^2 d + \langle \phi_s^2 \phi_d^2 \rangle (2|s|^2 d + s^2 d^*) \} \\ & - \gamma \left[ \frac{2\xi^4}{\eta_0} \langle \phi_d^2 (\hat{\mathbf{v}} \cdot \mathbf{q})^4 \rangle_d + \frac{1}{3\eta_0^5} \langle \phi_d^6 \rangle |d|^4 d - \frac{2\xi^2}{3\eta_0^3} \langle \phi_d^4 [4\{(\hat{\mathbf{v}} \cdot \mathbf{q})^2 d\} |d|^2 + d^2 \{(\hat{\mathbf{v}} \cdot \mathbf{q})^2 d\}^* \right. \\ & \left. - 2d|(\hat{\mathbf{v}} \cdot \mathbf{q})d|^2 + 3\{(\hat{\mathbf{v}} \cdot \mathbf{q})d\}^2 d^* \rangle \right] + O(\gamma^2) = 0, \end{aligned} \quad (2.7)$$

with  $\gamma = \alpha \ln(T_c/T)$ , the GL coherence length  $\xi = \{\beta v_F^2 / 6 \ln(T_c/T)\}^{1/2}$  and the energy gap in the absence of a magnetic field  $\eta_0 = \{\ln(T_c/T)/\beta\}^{1/2}$ . Because  $s(\mathbf{r})$  is in the order  $O(\gamma)$  as shown later in Eq. (2.26), the terms including  $s(\mathbf{r})$  are neglected among the correction terms of the order  $O(\gamma)$  in Eq. (2.7). The parameter  $c_s$  in Eq. (2.6) is defined by

$$c_s^{-1} \equiv \alpha \{ (N_F V_s)^{-1} - (N_F V_d)^{-1} - \ln(T_c/T) \} = \alpha \{ (N_F V_s)^{-1} - (N_F V_d)^{-1} \} + O(\gamma), \quad (2.8)$$

which depends on the interaction parameters  $V_s$  and  $V_d$ . From Eq. (2.8),  $c_s > 0$  in the case  $V_s$  is attractive and  $T > T_s$ . Here,  $T_s$  defined by  $(N_F V_s)^{-1} = \ln(2\omega_D \bar{\gamma}/\pi T_s)$  is the onset temperature of  $s$ -wave superconductivity in the hypothetical super-cooling state where  $d_{x^2-y^2}$ -wave superconductivity does not occur even at  $T \leq T_c$ . Our study is restricted in the temperature region  $T_s < T \leq T_c$ . On the other hand,  $c_s < 0$  in the case  $V_s$  is repulsive.

We note that, when the  $s$ -wave component  $V_s$  can be neglected in the pairing interaction (that is, in the limit  $V_s \rightarrow 0$ ),  $c_s \rightarrow 0$ . Then, the pure  $d_{x^2-y^2}$ -wave case is obtained. In the case  $c_s = 0$ , we recognize that  $s$ -wave component of the order parameter vanishes ( $s(\mathbf{r})=0$ ) from Eq. (2.6). Therefore, Eq. (2.7) is reduced to the one-component GL equation for only the  $d_{x^2-y^2}$ -wave component. There, the GL equation does not include the  $s$ -wave component, but includes the correction terms of the order  $O(\gamma)$ .

In order to calculate the upper critical magnetic field  $H_{c2}$  and the order parameter at  $H_{c2}$ , we consider the linearized GL equations. The annihilation and the creation operators are, respectively, introduced as  $a = -\epsilon^{-1/2}(q_x - iq_y)$  and  $a^\dagger = -\epsilon^{-1/2}(q_x + iq_y)$ , where  $\epsilon = 4\pi H/\phi_0 = 4\pi/a_x a_y$ . Then,

$$\hat{\mathbf{v}} \cdot \mathbf{q} = -\sqrt{\epsilon}(\hat{v}_+ a + \hat{v}_- a^\dagger) \quad (2.9)$$

with  $\hat{v}_\pm = (\hat{v}_x \pm i\hat{v}_y)/2 = e^{\pm i\theta}/2$ . By substituting Eq. (2.9) into Eqs. (2.6) and (2.7), the linearized GL equations are written as

$$\frac{1}{\eta_0} s + \gamma c_s \frac{2\epsilon\xi^2}{\eta_0} \{ \langle \phi_s^2 \hat{v}_+ \hat{v}_- \rangle [aa^\dagger] s + \langle \phi_s \phi_d \hat{v}_+^2 \rangle a^2 d + \langle \phi_s \phi_d \hat{v}_-^2 \rangle a^{\dagger 2} d \} + O(\gamma^2) = 0, \quad (2.10)$$

$$\begin{aligned} -\frac{1}{\eta_0} d + \frac{2\epsilon\xi^2}{\eta_0} \{ \langle \phi_d^2 \hat{v}_+ \hat{v}_- \rangle [aa^\dagger] d + \langle \phi_s \phi_d \hat{v}_+^2 \rangle a^2 s + \langle \phi_s \phi_d \hat{v}_-^2 \rangle a^{\dagger 2} s \} \\ - \gamma \frac{2\epsilon^2 \xi^4}{\eta_0} \{ \langle \phi_d^4 \hat{v}_+^4 \rangle a^4 d + \langle \phi_d^4 \hat{v}_-^4 \rangle a^{\dagger 4} d + \langle \phi_d^4 \hat{v}_+^2 \hat{v}_-^2 \rangle [a^2 a^{\dagger 2}] d \} + O(\gamma^2) = 0, \end{aligned} \quad (2.11)$$

where  $[a^m a^{\dagger n}]$  means to take all the permutations of the product, such as  $[aa^\dagger] = aa^\dagger + a^\dagger a$  or  $[a^2 a^{\dagger 2}] = a^2 a^{\dagger 2} + aa^\dagger aa^\dagger + a^\dagger a^2 a^\dagger + aa^\dagger a^2 a^\dagger + a^\dagger a a^\dagger a + a^{\dagger 2} a^2$ .

In the investigation of the vortex lattice state, it is convenient to use the magnetic Bloch state,<sup>21</sup>

$$\psi_n(\mathbf{r}|\mathbf{r}_0) = (\epsilon^n n!)^{-1/2} \partial_t^n \psi(\mathbf{r}|\mathbf{r}_0|t)|_{t=0}, \quad (2.12)$$

where

$$\psi(\mathbf{r}|\mathbf{r}_0|t) = \left( \frac{2a_y}{a_x} \right)^{1/4} \sum_p \exp \left[ \frac{2\pi}{a_x a_y} \left\{ -\frac{1}{2} (y + y_0 + p a_y - 2t)^2 + t^2 - i p a_y (x + x_0 + \frac{1}{2} \zeta p a_x) - i y_0 x \right\} \right]. \quad (2.13)$$

Here,  $n$  is the index of the Landau level, and there are relations  $a\psi_n = \sqrt{n}\psi_{n-1}$  and  $a^\dagger\psi_n = \sqrt{n+1}\psi_{n+1}$ . The function  $\psi_0(\mathbf{r}|\mathbf{r}_0)$  is the well-known Abrikosov solution of the vortex lattice.<sup>17,21</sup> In Eqs. (2.12) and (2.13),  $\mathbf{r}_0 = (x_0, y_0)$  is related to the quasi-momentum of the Bloch state, and determines the position of the vortex center. In our presentation of figures, we set  $\mathbf{r}_0 = -(\mathbf{r}_1 + \mathbf{r}_2)/2$  so that one of the vortex centers locates at the origin of the coordinate.

The order parameters can be expressed as the linear combination of the magnetic Bloch states as follows,

$$d(\mathbf{r}) = \sum_{n=0}^{\infty} d_n \psi_n(\mathbf{r}|\mathbf{r}_0), \quad s(\mathbf{r}) = \sum_{n=0}^{\infty} s_n \psi_n(\mathbf{r}|\mathbf{r}_0). \quad (2.14)$$

In the limit  $\gamma \rightarrow 0$  ( $T \rightarrow T_c$ ), Eqs. (2.10) and (2.11) are reduced to the form of the conventional GL equation. Therefore, the order parameters are given by the Abrikosov solution  $d(\mathbf{r}) = d_0 \psi_0(\mathbf{r}|\mathbf{r}_0)$  and  $s(\mathbf{r}) = 0$  at  $T \rightarrow T_c$ . On lowering temperature below  $T_c$ , the corrections of the order  $O(\gamma)$  are added to the Abrikosov solution. In order to investigate the corrections, the factors  $d_n$  and  $s_n$  (except for  $d_0$ ) are expanded in powers of  $\gamma$ ,

$$d_n = d_n^{(0)} + \gamma d_n^{(1)} + O(\gamma^2), \quad (n \neq 0) \quad s_n = s_n^{(0)} + \gamma s_n^{(1)} + O(\gamma^2). \quad (2.15)$$

Now, the upper critical field is given by  $\epsilon = 4\pi H_{c2}/\phi_0$  as the function of  $T$ . We also expand  $\epsilon$  in powers of  $\gamma$ ,

$$\epsilon \xi^2 = \epsilon^{(0)} \xi^2 + \gamma \epsilon^{(1)} \xi^2 + O(\gamma^2). \quad (2.16)$$

Equations (2.14)-(2.16) are substituted into Eqs. (2.10) and (2.11). At the order of  $O(1)$ , we obtain  $s_n^{(0)} = 0$  from Eq. (2.10), and

$$d_n^{(0)} - 2\epsilon^{(0)} \xi^2 \left\{ \langle \phi_d^2 \hat{v}_+ \hat{v}_- \rangle (2n+1) d_n^{(0)} + \langle \phi_s \phi_d \hat{v}_+^2 \rangle \sqrt{(n+2)(n+1)} s_{n+2}^{(0)} + \langle \phi_s \phi_d \hat{v}_-^2 \rangle \sqrt{n(n-1)} s_{n-2}^{(0)} \right\} = 0 \quad (2.17)$$

from Eq. (2.11). Equation (2.17) gives

$$\epsilon^{(0)} \xi^2 = \{ 2 \langle \phi_d^2 \hat{v}_+ \hat{v}_- \rangle \}^{-1} \quad (2.18)$$

for  $n = 0$ , and  $d_n^{(0)} = 0$  for  $n > 0$ . On the other hand, at the order of  $O(\gamma)$ , we obtain

$$s_n^{(1)} + c_s 2\epsilon^{(0)} \xi^2 \left\{ \langle \phi_s \phi_d \hat{v}_+^2 \rangle \sqrt{(n+2)(n+1)} d_{n+2}^{(0)} + \langle \phi_s \phi_d \hat{v}_-^2 \rangle \sqrt{n(n-1)} d_{n-2}^{(0)} \right\} = 0, \quad (2.19)$$

from Eq. (2.10), and

$$\begin{aligned} & \left\{ 1 - 2\epsilon^{(0)} \xi^2 \langle \phi_d^2 \hat{v}_+ \hat{v}_- \rangle (2n+1) \right\} d_n^{(1)} - 2\epsilon^{(1)} \xi^2 \langle \phi_d^2 \hat{v}_+ \hat{v}_- \rangle d_n^{(0)} \\ & - 2\epsilon^{(0)} \xi^2 \left\{ \langle \phi_s \phi_d \hat{v}_+^2 \rangle \sqrt{(n+2)(n+1)} s_{n+2}^{(1)} + \langle \phi_s \phi_d \hat{v}_-^2 \rangle \sqrt{n(n-1)} s_{n-2}^{(1)} \right\} \\ & + 2(\epsilon^{(0)})^2 \xi^4 \left\{ \langle \phi_d^2 \hat{v}_+^4 \rangle \sqrt{(n+4)(n+3)(n+2)(n+1)} d_{n+4}^{(0)} + \langle \phi_d^2 \hat{v}_-^4 \rangle \sqrt{n(n-1)(n-2)(n-3)} d_{n-4}^{(0)} \right. \\ & \left. + \langle \phi_d^2 \hat{v}_+^2 \hat{v}_-^2 \rangle 3(2n^2 + 2n + 1) d_n^{(0)} \right\} = 0 \end{aligned} \quad (2.20)$$

from Eq. (2.11). Equation (2.19) gives

$$s_2^{(1)} = -\sqrt{2} c_s \frac{\langle \phi_s \phi_d \hat{v}_-^2 \rangle}{\langle \phi_d^2 \hat{v}_+ \hat{v}_- \rangle} d_0 \quad (2.21)$$

for  $n = 2$ , and  $s_n^{(1)} = 0$  for  $n \neq 2$ . From Eq. (2.20), we obtain

$$\frac{\epsilon^{(1)}}{\epsilon^{(0)}} = \frac{3\langle \phi_d^2 \hat{v}_+^2 \hat{v}_-^2 \rangle}{2\langle \phi_d^2 \hat{v}_+ \hat{v}_- \rangle^2} + 2c_s \frac{\langle \phi_s \phi_d \hat{v}_+^2 \rangle \langle \phi_s \phi_d \hat{v}_-^2 \rangle}{\langle \phi_d^2 \hat{v}_+ \hat{v}_- \rangle^2} \quad (2.22)$$

for  $n = 0$ ,

$$d_4^{(1)} = \frac{\sqrt{6}}{8} \left( \frac{\langle \phi_d^2 \hat{v}_-^4 \rangle}{\langle \phi_d^2 \hat{v}_+ \hat{v}_- \rangle^2} + 2c_s \frac{\langle \phi_s \phi_d \hat{v}_-^2 \rangle^2}{\langle \phi_d^2 \hat{v}_+ \hat{v}_- \rangle^2} \right) d_0 \quad (2.23)$$

for  $n = 4$ , and  $d_n^{(1)} = 0$  for  $n \neq 0, 4$ .

As a result,  $H_{c2}$  is given as

$$\epsilon = \frac{4\pi H_{c2}}{\phi_0} = \frac{1}{2\langle \phi_d^2 \hat{v}_+ \hat{v}_- \rangle \xi^2} \left\{ 1 + \gamma \frac{\epsilon^{(1)}}{\epsilon^{(0)}} + O(\gamma^2) \right\} \quad (2.24)$$

with the use of  $\epsilon^{(1)}/\epsilon^{(0)}$  in Eq. (2.22). The order parameters at  $H_{c2}$  are given by

$$d(\mathbf{r}) = d_0 \psi_0(\mathbf{r}|\mathbf{r}_0) + \gamma d_4^{(1)} \psi_4(\mathbf{r}|\mathbf{r}_0) + O(\gamma^2), \quad (2.25)$$

$$s(\mathbf{r}) = \gamma s_2^{(1)} \psi_2(\mathbf{r}|\mathbf{r}_0) + O(\gamma^2), \quad (2.26)$$

with the use of  $d_4^{(1)}$  in Eq. (2.23) and  $s_2^{(1)}$  in Eq. (2.21).

Here, the  $\theta$ -integral is performed with adopting the forms of  $\phi_d$  and  $\phi_s$  in Eq. (2.2). The values of  $\langle \dots \rangle$  appearing in this paper are evaluated as follows,

$$\begin{aligned} \langle \phi_d^2 \hat{v}_+ \hat{v}_- \rangle &= \frac{1}{4}, & \langle \phi_d^2 \hat{v}_+^2 \hat{v}_-^2 \rangle &= \frac{1}{16}, & \langle \phi_d^2 \hat{v}_-^4 \rangle &= \frac{1}{32} e^{-4i\theta_0}, \\ \langle \phi_s \phi_d \hat{v}_+^2 \rangle &= \frac{1}{4\sqrt{2}} e^{2i\theta_0}, & \langle \phi_s \phi_d \hat{v}_-^2 \rangle &= \frac{1}{4\sqrt{2}} e^{-2i\theta_0}, & \langle \phi_d^4 \rangle &= \frac{3}{2}, & \langle \phi_d^4 \hat{v}_+ \hat{v}_- \rangle &= \frac{3}{8}. \end{aligned} \quad (2.27)$$

Therefore, Eqs. (2.24)-(2.26) are reduced to

$$\epsilon = \frac{4\pi H_{c2}}{\phi_0} = \frac{2}{\xi^2} \left\{ 1 + \gamma \left( \frac{3}{2} + c_s \right) + O(\gamma^2) \right\}, \quad (2.28)$$

$$d(\mathbf{r}) = d_0 \left\{ \psi_0(\mathbf{r}|\mathbf{r}_0) + \frac{\sqrt{6}}{8} \gamma \left( \frac{1}{2} + c_s \right) e^{-4i\theta_0} \psi_4(\mathbf{r}|\mathbf{r}_0) + O(\gamma^2) \right\}, \quad (2.29)$$

$$s(\mathbf{r}) = d_0 \{ -\gamma c_s e^{-2i\theta_0} \psi_2(\mathbf{r}|\mathbf{r}_0) + O(\gamma^2) \}. \quad (2.30)$$

In the correction terms of the order  $O(\gamma)$  in Eqs. (2.28)-(2.30), the terms without  $c_s$  comes from the correction terms of the GL equation, that is, the  $A_4$ -terms in Eq. (2.4), which has been neglected so far in the conventional GL theory. The terms proportional to  $c_s$  comes from the induced  $s$ -wave order parameter. As shown in Eq. (2.30), the effect of the induced  $s$ -wave component appears in the order  $O(\gamma)$ . It corresponds to the result  $d(\mathbf{r})/s(\mathbf{r}) \sim 1 - T/T_c$  suggested by the two-component GL theory.<sup>8</sup> From Eq. (2.29), we recognize that the correction of the  $d_{x^2-y^2}$ -wave superconductivity also appears in the same order of the induced  $s$ -wave component.

For comparison, by exchanging  $\phi_s \leftrightarrow \phi_d$  and putting  $c_s = 0$ , we consider the case of an isotropic  $s$ -wave superconductor without the  $s$ - $d$  mixing. The corresponding  $\theta$ -integrated values are evaluated as follows,

$$\langle \phi_s^2 \hat{v}_+ \hat{v}_- \rangle = \frac{1}{4}, \quad \langle \phi_s^2 \hat{v}_+^2 \hat{v}_-^2 \rangle = \frac{1}{16}, \quad \langle \phi_s^2 \hat{v}_-^4 \rangle = 0, \quad \langle \phi_s^4 \rangle = 1, \quad \langle \phi_s^4 \hat{v}_+ \hat{v}_- \rangle = \frac{1}{4}. \quad (2.31)$$

In this case, from Eq. (2.31),  $H_{c2}$  is written as the same form of Eq. (2.28) ( $c_s=0$ ) even in an isotropic  $s$ -wave superconductor within the order  $O(\gamma)$ . On the other hand, from Eq. (2.31), the order parameter have the form  $s(\mathbf{r}) = s_0 \psi_0(\mathbf{r}|\mathbf{r}_0)$ , that is, the fourth Landau level function  $\psi_4(\mathbf{r}|\mathbf{r}_0)$  does not appear in an isotropic  $s$ -wave case.

Then, it is noted that the appearance of  $\psi_4(\mathbf{r}|\mathbf{r}_0)$  is the characteristic feature of the  $d_{x^2-y^2}$ -wave superconductor's vortex lattice. From Eq. (2.29), we see that the induced  $s$ -wave order parameter enhances the weight of  $\psi_4(\mathbf{r}|\mathbf{r}_0)$  term in the case  $V_s$  is attractive ( $c_s > 0$ ). On the other hand, the weight of  $\psi_4(\mathbf{r}|\mathbf{r}_0)$  term is suppressed in the case  $V_s$  is repulsive ( $c_s < 0$ ). The higher Landau level functions,  $\psi_8(\mathbf{r}|\mathbf{r}_0)$ ,  $\psi_{12}(\mathbf{r}|\mathbf{r}_0)$ ,  $\dots$ , also appear in higher orders of  $\gamma$ . For example, the eighth Landau level function  $\psi_8(\mathbf{r}|\mathbf{r}_0)$  appears in the order  $O(\gamma^2)$ .

As is seen from Eq. (2.28),  $H_{c2}$  is enhanced by the induced  $s$ -wave order parameter in the case  $V_s$  is attractive, which is consistent with the result of Franz *et al.* (Fig. 9 of Ref. 8). On the other hand,  $H_{c2}$  is suppressed in the case  $V_s$  is repulsive, which is consistent with the result of Won and Maki (Fig. 1 of Ref. 23).

If we set  $\xi^{-2} \sim \Delta t$  with  $\Delta t = 1 - T/T_c$  in Eq. (2.28), we obtain the result corresponding to that of Franz *et al.*<sup>8</sup> There, the induced  $s$ -wave order parameter leads an upward curvature in the curve of  $H_{c2}(T)$  near  $T_c$ , since the factor of  $(\Delta t)^2$  is positive in  $H_{c2}$ . However, this upward curvature occurs even in the pure  $d_{x^2-y^2}$ -wave case ( $c_s = 0$ ) because of  $\frac{3}{2}\gamma$  in Eq. (2.28), which is neglected in the study of Franz *et al.* but derived from the  $O(\gamma)$  correction of the  $d_{x^2-y^2}$ -wave superconductivity. This upward curvature by  $\frac{3}{2}\gamma$  occurs even in an isotropic  $s$ -wave superconductor in this approximation. These unexpected results are modified as follows by a careful consideration. Exactly speaking,  $\xi^{-2} \sim T^2 \ln(T_c/T)$  should be expanded as  $\xi^{-2} \sim \Delta t - \frac{3}{2}(\Delta t)^2$ . Thus, we obtain

$$\epsilon = \frac{4\pi H_{c2}}{\phi_0} \sim \Delta t + \left\{ c_s - \frac{3}{2}(1 - \alpha) \right\} (\Delta t)^2. \quad (2.32)$$

Now, in the pure  $d_{x^2-y^2}$ -wave case and the isotropic  $s$ -wave case ( $c_s = 0$ ), the factor of  $(\Delta t)^2$  is negative and the curve of  $H_{c2}(T)$  shows a downward curvature near  $T_c$ . For  $c_s > \frac{3}{2}(1 - \alpha)$ , the factor of  $(\Delta t)^2$  changes to positive and the curve of  $H_{c2}(T)$  shows an upward curvature.

As is seen from Eq. (2.21), the amplitude of the induced  $s$ -wave order parameter is determined by not only the parameter of the gradient coupling between  $d_{x^2-y^2}$ - and  $s$ -wave order parameters,  $\langle \phi_s \phi_d \hat{v}_-^2 \rangle$ , but also the parameter of the pairing interaction,  $c_s$  defined in Eq. (2.8). The amplitude of the induced  $s$ -wave order parameter is proportional to the product of both parameters.

From Eq. (2.26), the spatial variation of the induced  $s$ -wave order parameter has the same structure as that of the second Landau level function  $\psi_2(\mathbf{r}|\mathbf{r}_0)$ . Figure 2 is the case of a square lattice ( $a_y/a_x = 0.5$ ,  $\zeta = 0.5$ ). In Fig. 2 (a), we show the amplitude of the induced  $s$ -wave order parameter,  $|s(\mathbf{r})/\gamma s_2^{(1)}| = |\psi_2(\mathbf{r}|\mathbf{r}_0)|$ . The amplitude is suppressed near the vortex of the induced  $s$ -wave order parameter. To show it clearly, we schematically present the position of the vortices and the winding number of their phase in Fig. 2 (b). At the vortex center of the  $d_{x^2-y^2}$ -wave superconductivity (its winding number is +1), the induced  $s$ -wave order parameter has a vortex with the winding number -1. It is consistent with the result of the single vortex case.<sup>7,8,10,11,13,14</sup> Further, the  $s$ -wave order parameter has extra vortices with the winding number +2, which locates at the farthest points from the vortices of the  $d_{x^2-y^2}$ -wave superconductivity. In total, we obtain the winding number +1 for the phase of the  $s$ -wave order parameter when we go round about the boundary of a unit cell in the vortex lattice. The amplitude and the winding number of the  $s$ -wave order parameter are not affected by the orientation  $\theta_0$  of the vortex lattice. Figure 3 is the case of an oblique lattice with  $73^\circ$  ( $a_y/a_x = 0.676$ ,  $\zeta = 0.5$ ). In Fig. 3 (a), we show the amplitude of the induced  $s$ -wave order parameter, which is consistent with the result of Berlinsky *et al.* (Fig. 3 (b) in Ref. 7. The  $a$  axis and the  $b$  axis are exchanged each other in our calculation.) The corresponding position of the vortices and their winding number are shown in Fig. 3 (b). In the oblique lattice case, the vortex with the winding number +2 in the square lattice

case splits into two vortices with the winding number +1. In the limit of a triangular lattice, these vortices with the winding number +1 locates at the farthest points from the vortices of the  $d_{x^2-y^2}$ -wave superconductivity.

The spatial variation of the  $d_{x^2-y^2}$ -wave order parameter in Eq. (2.29) is presented later in Sec. V.

### III. CURRENT AND MAGNETIC FIELD

We calculate the current and its induced magnetic field around vortices near  $H_{c2}$ . Magnetic field  $\mathbf{H}(\mathbf{r})$  is divided into an external field  $\mathbf{H}_0 = (0, 0, H_0)$  and an internal field  $\mathbf{h}(\mathbf{r})$  which is induced by the current  $\mathbf{j}(\mathbf{r})$ ,

$$\mathbf{H}(\mathbf{r}) = \mathbf{H}_0 + \mathbf{h}(\mathbf{r}). \quad (3.1)$$

Amplitude of the order parameter is small near  $H_{c2}$ . Therefore, as for the current and magnetic field, we consider terms up to the order  $O(|d_0|^2)$ . The expression for the current density is derived as follows from the Gor'kov equation with including the correction terms of the order  $O(\gamma)$  (As for the detail of the derivation, see Appendix A of Ref. 19.),

$$\mathbf{j}(\mathbf{r}) \equiv \xi \nabla \times \mathbf{H}(\mathbf{r}) / (\phi_0 / \xi^2) = \xi \nabla \times \mathbf{h}(\mathbf{r}) / (\phi_0 / \xi^2) \quad (3.2)$$

$$= -\frac{2\pi}{\kappa^2 \eta_0^2} \left[ \xi \langle \hat{\mathbf{v}} \{ (\hat{\mathbf{v}} \cdot \mathbf{q}) \Delta(\mathbf{r}, \theta) \} \Delta^*(\mathbf{r}, \theta) \rangle \right. \\ \left. - \gamma \xi^3 \left\{ \langle \hat{\mathbf{v}} \{ (\hat{\mathbf{v}} \cdot \mathbf{q})^3 \Delta(\mathbf{r}, \theta) \} \Delta^*(\mathbf{r}, \theta) \rangle + \langle \hat{\mathbf{v}} \{ (\hat{\mathbf{v}} \cdot \mathbf{q})^2 \Delta(\mathbf{r}, \theta) \} \{ (\hat{\mathbf{v}} \cdot \mathbf{q}) \Delta(\mathbf{r}, \theta) \}^* \rangle \right\} + O(\gamma^2) \right] + \text{c.c.}, \quad (3.3)$$

where terms with  $|\Delta|^4$  (that is, terms in the order  $O(|d_0|^4)$ ) are neglected. In Eq. (3.3),

$$\kappa^{-2} = \frac{4|e|N_F v_F^2 \beta \xi^2 \eta_0^2}{3c\phi_0} = \frac{3}{8\pi^2} \left( \frac{T_c}{T} \right)^2 \kappa_{\text{GL}}^{-2}, \quad (3.4)$$

where the GL parameter  $\kappa_{\text{GL}}$  is given by

$$\kappa_{\text{GL}} = \frac{9}{7\pi\zeta(3)N_F} \left( \frac{\hbar c}{|e|} \right)^2 \frac{(\pi k_B T_c)^2}{(\hbar v_F)^4}. \quad (3.5)$$

With the substitution of Eqs. (2.1), (2.9) and (2.14) into Eq. (3.3), the current density is written as

$$\mathbf{j}(\mathbf{r}) = \frac{2\pi\sqrt{\epsilon\xi^2}}{\kappa^2\eta_0^2} \sum_{n_1, n_2} (\mathbf{j})_{n_1, n_2} \psi_{n_1}(\mathbf{r}|\mathbf{r}_0) \psi_{n_2}^*(\mathbf{r}|\mathbf{r}_0), \quad (3.6)$$

where

$$\begin{aligned} (\mathbf{j})_{n_1, n_2} = & \langle \phi_d^2 \hat{\mathbf{v}} \hat{v}_+ \rangle (\sqrt{n_1+1} d_{n_1+1} d_{n_2}^* + \sqrt{n_2} d_{n_1} d_{n_2-1}^*) + \langle \phi_d^2 \hat{\mathbf{v}} \hat{v}_- \rangle (\sqrt{n_1} d_{n_1-1} d_{n_2}^* + \sqrt{n_2+1} d_{n_1} d_{n_2+1}^*) \\ & + \langle \phi_s^2 \hat{\mathbf{v}} \hat{v}_+ \rangle (\sqrt{n_1+1} s_{n_1+1} s_{n_2}^* + \sqrt{n_2} s_{n_1} s_{n_2-1}^*) + \langle \phi_s^2 \hat{\mathbf{v}} \hat{v}_- \rangle (\sqrt{n_1} s_{n_1-1} s_{n_2}^* + \sqrt{n_2+1} s_{n_1} s_{n_2+1}^*) \\ & + \langle \phi_s \phi_d \hat{\mathbf{v}} \hat{v}_+ \rangle (\sqrt{n_1+1} s_{n_1+1} d_{n_2}^* + \sqrt{n_2} s_{n_1} d_{n_2-1}^* + \sqrt{n_1+1} d_{n_1+1} s_{n_2}^* + \sqrt{n_2} d_{n_1} s_{n_2-1}^*) \\ & + \langle \phi_s \phi_d \hat{\mathbf{v}} \hat{v}_- \rangle (\sqrt{n_1} s_{n_1-1} d_{n_2}^* + \sqrt{n_2+1} s_{n_1} d_{n_2+1}^* + \sqrt{n_1} d_{n_1-1} s_{n_2}^* + \sqrt{n_2+1} d_{n_1} s_{n_2+1}^*) \\ & - \gamma \epsilon \xi^2 \left\{ \langle \phi_d^2 \hat{\mathbf{v}} \hat{v}_+^3 \rangle \left( \sqrt{(n_1+3)(n_1+2)(n_1+1)} d_{n_1+3} d_{n_2}^* + \sqrt{n_2(n_2-1)(n_2-2)} d_{n_1} d_{n_2-3}^* \right. \right. \\ & \left. \left. + \sqrt{(n_1+2)(n_1+1)n_2} d_{n_1+2} d_{n_2-1}^* + \sqrt{(n_1+1)n_2(n_2-1)} d_{n_1+1} d_{n_2-2}^* \right) \right. \\ & + \langle \phi_d^2 \hat{\mathbf{v}} \hat{v}_-^3 \rangle \left( \sqrt{n_1(n_1-1)(n_1-2)} d_{n_1-3} d_{n_2}^* + \sqrt{(n_2+3)(n_2+2)(n_2+1)} d_{n_1} d_{n_2+3}^* \right. \\ & \left. + \sqrt{n_1(n_1-1)(n_2+1)} d_{n_1-2} d_{n_2+1}^* + \sqrt{n_1(n_2+2)(n_2+1)} d_{n_1-1} d_{n_2+2}^* \right) \\ & + \langle \phi_d^2 \hat{\mathbf{v}} \hat{v}_+^2 \hat{v}_- \rangle \left( (3n_1+2n_2+4) \sqrt{n_1+1} d_{n_1+1} d_{n_2}^* + (2n_1+3n_2+1) \sqrt{n_2} d_{n_1} d_{n_2-1}^* \right. \\ & \left. + \sqrt{(n_1+2)(n_1+1)(n_2+1)} d_{n_1+2} d_{n_2+1}^* + \sqrt{n_1 n_2 (n_2-1)} d_{n_1-1} d_{n_2-2}^* \right) \\ & \left. + \langle \phi_d^2 \hat{\mathbf{v}} \hat{v}_+ \hat{v}_-^2 \rangle \left( (3n_1+2n_2+1) \sqrt{n_1} d_{n_1-1} d_{n_2}^* + (2n_1+3n_2+4) \sqrt{n_2+1} d_{n_1} d_{n_2+1}^* \right. \right. \\ & \left. \left. + \sqrt{n_1(n_1-1)n_2} d_{n_1-2} d_{n_2-1}^* + \sqrt{(n_1+1)(n_2+2)(n_2+1)} d_{n_1+1} d_{n_2+2}^* \right) \right\} + O(\gamma^2). \end{aligned} \quad (3.7)$$



Among the correction terms of the order  $O(\gamma)$  in Eq. (3.7), we neglect the terms including  $s_n$ , since  $s_n$  is in the order  $O(\gamma)$  as shown in Eq. (2.26). Equation (3.7) satisfies a relation

$$(\mathbf{j})_{n_2, n_1} = \{(\mathbf{j})_{n_1, n_2}\}^*, \quad (3.8)$$

which ensures that  $\mathbf{j}(\mathbf{r})$  is real. By substituting the results of  $\epsilon$  and the order parameters  $d_n$  and  $s_n$  in Sec II [Eqs. (2.15), (2.16), (2.18) and (2.21)-(2.23)] into Eq. (3.7) and by introducing

$$j_{\pm} = (j_x \pm ij_y)/2, \quad (3.9)$$

we obtain

$$\begin{aligned} (j_+)_{1,0} &= \langle \phi_d^2 \hat{v}_+ \hat{v}_- \rangle |d_0|^2 + \gamma \left( \langle \phi_s \phi_d \hat{v}_+^2 \rangle \sqrt{2} s_2^{(1)} d_0^* - \epsilon^{(0)} \xi^2 \langle \phi_d^2 \hat{v}_+^2 \hat{v}_-^2 \rangle 4 |d_0|^2 \right) \\ &= \langle \phi_d^2 \hat{v}_+ \hat{v}_- \rangle \left\{ 1 - 2\gamma \left( \frac{\langle \phi_d^2 \hat{v}_+^2 \hat{v}_-^2 \rangle}{\langle \phi_d^2 \hat{v}_+ \hat{v}_- \rangle^2} + c_s \frac{\langle \phi_s \phi_d \hat{v}_+^2 \rangle \langle \phi_s \phi_d \hat{v}_-^2 \rangle}{\langle \phi_d^2 \hat{v}_+ \hat{v}_- \rangle^2} \right) + O(\gamma^2) \right\} |d_0|^2, \end{aligned} \quad (3.10)$$

$$\begin{aligned} (j_-)_{3,0} &= \gamma \left( \langle \phi_d^2 \hat{v}_+ \hat{v}_- \rangle 2d_4^{(1)} d_0^* + \langle \phi_s \phi_d \hat{v}_-^2 \rangle \sqrt{3} s_2^{(1)} d_0^* - \epsilon^{(0)} \xi^2 \langle \phi_d^2 \hat{v}_-^4 \rangle \sqrt{6} |d_0|^2 \right) \\ &= \langle \phi_d^2 \hat{v}_+ \hat{v}_- \rangle \left\{ -\frac{\sqrt{6}}{4} \gamma \left( \frac{\langle \phi_d^2 \hat{v}_-^4 \rangle}{\langle \phi_d^2 \hat{v}_+ \hat{v}_- \rangle^2} + 2c_s \frac{\langle \phi_s \phi_d \hat{v}_-^2 \rangle^2}{\langle \phi_d^2 \hat{v}_+ \hat{v}_- \rangle^2} \right) + O(\gamma^2) \right\} |d_0|^2, \end{aligned} \quad (3.11)$$

$$\begin{aligned} (j_+)_{5,0} &= \gamma \langle \phi_d^2 \hat{v}_+ \hat{v}_- \rangle \sqrt{5} d_4^{(1)} d_0^* \\ &= \langle \phi_d^2 \hat{v}_+ \hat{v}_- \rangle \left\{ \frac{\sqrt{30}}{8} \gamma \left( \frac{\langle \phi_d^2 \hat{v}_-^4 \rangle}{\langle \phi_d^2 \hat{v}_+ \hat{v}_- \rangle^2} + 2c_s \frac{\langle \phi_s \phi_d \hat{v}_-^2 \rangle^2}{\langle \phi_d^2 \hat{v}_+ \hat{v}_- \rangle^2} \right) + O(\gamma^2) \right\} |d_0|^2, \end{aligned} \quad (3.12)$$

$$\begin{aligned} (j_+)_{2,1} &= \gamma \left( \langle \phi_s \phi_d \hat{v}_+^2 \rangle s_2^{(1)} d_0^* - \epsilon^{(0)} \xi^2 \langle \phi_d^2 \hat{v}_+^2 \hat{v}_-^2 \rangle \sqrt{2} |d_0|^2 \right) \\ &= \langle \phi_d^2 \hat{v}_+ \hat{v}_- \rangle \left\{ -\frac{\sqrt{2}}{2} \gamma \left( \frac{\langle \phi_d^2 \hat{v}_+^2 \hat{v}_-^2 \rangle}{\langle \phi_d^2 \hat{v}_+ \hat{v}_- \rangle^2} + 2c_s \frac{\langle \phi_s \phi_d \hat{v}_+^2 \rangle \langle \phi_s \phi_d \hat{v}_-^2 \rangle}{\langle \phi_d^2 \hat{v}_+ \hat{v}_- \rangle^2} \right) + O(\gamma^2) \right\} |d_0|^2, \end{aligned} \quad (3.13)$$

$$\begin{aligned} (j_-)_{4,1} &= \gamma \langle \phi_d^2 \hat{v}_+ \hat{v}_- \rangle \sqrt{5} d_4^{(1)} d_0^* \\ &= \langle \phi_d^2 \hat{v}_+ \hat{v}_- \rangle \left\{ \frac{\sqrt{6}}{8} \gamma \left( \frac{\langle \phi_d^2 \hat{v}_-^4 \rangle}{\langle \phi_d^2 \hat{v}_+ \hat{v}_- \rangle^2} + 2c_s \frac{\langle \phi_s \phi_d \hat{v}_-^2 \rangle^2}{\langle \phi_d^2 \hat{v}_+ \hat{v}_- \rangle^2} \right) + O(\gamma^2) \right\} |d_0|^2. \end{aligned} \quad (3.14)$$

The other components  $(j_{\pm})_{n_1, n_2}$  for  $n_1 \geq n_2$  are zero within the order  $O(\gamma)$ . As a result, from Eqs. (3.8) and (3.9), the current density is given as follows by using Eqs. (3.10) - (3.14),

$$j_x = 2\text{Re}\{(j_+)_{1,0}\psi_1\psi_0^* + (j_-)_{3,0}\psi_3\psi_0^* + (j_+)_{5,0}\psi_5\psi_0^* + (j_+)_{2,1}\psi_2\psi_1^* + (j_-)_{4,1}\psi_4\psi_1^*\}, \quad (3.15)$$

$$j_y = 2\text{Im}\{-(j_+)_{1,0}\psi_1\psi_0^* + (j_-)_{3,0}\psi_3\psi_0^* - (j_+)_{5,0}\psi_5\psi_0^* - (j_+)_{2,1}\psi_2\psi_1^* + (j_-)_{4,1}\psi_4\psi_1^*\}. \quad (3.16)$$

The magnetic field induced by the current is obtained from the Maxwell equation. When we neglect terms of the order  $O(|d_0|^4)$ , the induced magnetic field  $\mathbf{h}(\mathbf{r})$  has the following form,

$$\mathbf{h}(\mathbf{r}) = \sum_{n_1, n_2} (\mathbf{h})_{n_1, n_2} \psi_{n_1}(\mathbf{r}|\mathbf{r}_0) \psi_{n_2}^*(\mathbf{r}|\mathbf{r}_0), \quad (3.17)$$

where  $(\mathbf{h})_{n_1, n_2}$  satisfies a relation

$$(\mathbf{h})_{n_2, n_1} = \{(\mathbf{h})_{n_1, n_2}\}^* \quad (3.18)$$

for  $\mathbf{h}(\mathbf{r})$  to be real. In our case,  $\mathbf{h}(\mathbf{r})$  has only the  $z$ -component,  $\mathbf{h}(\mathbf{r}) = (0, 0, h_z(\mathbf{r}))$ .

From the Maxwell equation (3.2), we have relations

$$(j_+)_{n_1, n_2} = \frac{\sqrt{\epsilon\xi^2}}{2} \frac{\xi^2}{\phi_0} \left\{ -\sqrt{n_1}(h_z)_{n_1-1, n_2} + \sqrt{n_2+1}(h_z)_{n_1, n_2+1} \right\}, \quad (3.19)$$

$$(j_-)_{n_1, n_2} = \frac{\sqrt{\epsilon\xi^2}}{2} \frac{\xi^2}{\phi_0} \left\{ \sqrt{n_1+1}(h_z)_{n_1+1, n_2} - \sqrt{n_2}(h_z)_{n_1, n_2-1} \right\}. \quad (3.20)$$

We also have a relation

$$\sqrt{n_1+1}(j_+)_{n_1+1, n_2} + \sqrt{n_1}(j_-)_{n_1-1, n_2} - \sqrt{n_2+1}(j_-)_{n_1, n_2+1} - \sqrt{n_2}(j_+)_{n_1, n_2-1} = 0 \quad (3.21)$$

from  $\text{div} \mathbf{j} = 0$ . Therefore,  $(h_z)_{n_1, n_2}$  is written as follows from Eqs. (3.10)-(3.14) and (3.19)-(3.21),

$$(h_z)_{0,0} = -\frac{2}{\sqrt{\epsilon\xi^2}} \frac{\phi_0}{\xi^2} \sum_{n=1}^{\infty} \frac{1}{\sqrt{n}} (j_+)_{n, n-1} = h_z^{(0)} + \gamma(h_z^{(1)})_{0,0} + O(\gamma^2), \quad (3.22)$$

$$(h_z)_{1,1} = -\frac{2}{\sqrt{\epsilon\xi^2}} \frac{\phi_0}{\xi^2} \sum_{n=2}^{\infty} \frac{1}{\sqrt{n}} (j_+)_{n, n-1} = \gamma(h_z^{(1)})_{1,1} + O(\gamma^2), \quad (3.23)$$

$$(h_z)_{4,0} = -\frac{2}{\sqrt{\epsilon\xi^2}} \frac{\phi_0}{\xi^2} \left\{ -\frac{1}{2}(j_-)_{3,0} \right\} = \gamma(h_z^{(1)})_{4,0} + O(\gamma^2), \quad (3.24)$$

where

$$h_z^{(0)} = -\frac{4\pi \langle \phi_d^2 \hat{v}_+ \hat{v}_- \rangle}{\kappa^2 \eta_0^2} |d_0|^2, \quad (< 0) \quad (3.25)$$

$$\frac{(h_z^{(1)})_{0,0}}{h_z^{(0)}} = -\left( \frac{5 \langle \phi_d^2 \hat{v}_+^2 \hat{v}_-^2 \rangle}{2 \langle \phi_d^2 \hat{v}_+ \hat{v}_- \rangle^2} + 3c_s \frac{\langle \phi_s \phi_d \hat{v}_+^2 \rangle \langle \phi_s \phi_d \hat{v}_-^2 \rangle}{\langle \phi_d^2 \hat{v}_+ \hat{v}_- \rangle^2} \right), \quad (3.26)$$

$$\frac{(h_z^{(1)})_{1,1}}{h_z^{(0)}} = -\left( \frac{\langle \phi_d^2 \hat{v}_+^2 \hat{v}_-^2 \rangle}{2 \langle \phi_d^2 \hat{v}_+ \hat{v}_- \rangle^2} + c_s \frac{\langle \phi_s \phi_d \hat{v}_+^2 \rangle \langle \phi_s \phi_d \hat{v}_-^2 \rangle}{\langle \phi_d^2 \hat{v}_+ \hat{v}_- \rangle^2} \right), \quad (3.27)$$

$$\frac{(h_z^{(1)})_{4,0}}{h_z^{(0)}} = \frac{\sqrt{6}}{8} \left( \frac{\langle \phi_d^2 \hat{v}_-^4 \rangle}{\langle \phi_d^2 \hat{v}_+ \hat{v}_- \rangle^2} + 2c_s \frac{\langle \phi_s \phi_d \hat{v}_-^2 \rangle^2}{\langle \phi_d^2 \hat{v}_+ \hat{v}_- \rangle^2} \right). \quad (3.28)$$

The other components  $(h_z)_{n_1, n_2}$  for  $n_1 \geq n_2$  vanish within the order  $O(\gamma)$ . As a result, the induced magnetic field is written as

$$h_z(\mathbf{r}) = \left\{ h_z^{(0)} + \gamma(h_z^{(1)})_{0,0} \right\} |\psi_0|^2 + \gamma(h_z^{(1)})_{1,1} |\psi_1|^2 + 2\gamma \text{Re} \left\{ (h_z^{(1)})_{4,0} \psi_4 \psi_0^* \right\} + O(\gamma^2). \quad (3.29)$$

By using the  $\theta$ -integrated values in Eq. (2.27),  $h_z(\mathbf{r})$  in Eq. (3.29) is reduced to

$$h_z(\mathbf{r}) = h_z^{(0)} \left[ \left\{ 1 - \frac{5}{2}\gamma \left( 1 + \frac{3}{5}c_s \right) \right\} |\psi_0|^2 - \frac{1}{2}\gamma(1+c_s) |\psi_1|^2 + \frac{\sqrt{6}}{8}\gamma(1+2c_s) \text{Re} \left\{ e^{-4i\theta_0} \psi_4 \psi_0^* \right\} + O(\gamma^2) \right]. \quad (3.30)$$

The spatial variation of the magnetic field in Eq. (3.30) is presented later in Sec. V.

When we consider the case of an isotropic  $s$ -wave superconductor without the  $s$ - $d$  mixing ( $\phi_s \leftrightarrow \phi_d$ ,  $c_s = 0$ ), by using Eqs. (2.31) we obtain

$$h_z(\mathbf{r}) = h_z^{(0)} \left\{ \left( 1 - \frac{5}{2}\gamma \right) |\psi_0|^2 - \frac{1}{2}\gamma |\psi_1|^2 + O(\gamma^2) \right\}, \quad (3.31)$$

where  $(h_z^{(1)})_{4,0}$  vanishes. From the comparison between Eqs. (3.30) and (3.31), it is concluded that the appearance of the  $\psi_4 \psi_0^*$  term in the magnetic field distribution is the characteristic feature of the  $d_{x^2-y^2}$ -wave superconductor's vortex lattice. As is seen from Eq. (3.30), the contribution of the  $\psi_4 \psi_0^*$  term is enhanced by the induced  $s$ -wave order parameter in the case  $V_s$  is attractive ( $c_s > 0$ ). On the other hand, its contribution is suppressed in the case  $V_s$  is repulsive ( $c_s < 0$ ).

#### IV. ORIENTATION AND UNIT CELL SHAPE OF THE VORTEX LATTICE

To know the equilibrium state of the vortex lattice, we search the free energy minimum about the orientation and the unit cell shape of the vortex lattice in the vicinity of  $H_{c2}$ . The free energy  $F$  is calculated by following the method of Abrikosov<sup>17</sup> and Takanaka.<sup>22</sup> As a result, the free energy of the vortex lattice is written as follows (the detailed derivation is given in Appendix A),

$$\frac{F}{F_0} = \kappa^2 \frac{\mathbf{B}^2}{(\phi_0/\xi^2)^2} - \frac{\left\{ \kappa^2 \frac{(\mathbf{B} - \mathbf{H}_{c2}) \cdot \bar{\mathbf{h}}}{(\phi_0/\xi^2)^2 |d_0|^2} \right\}^2}{\kappa^2 \frac{\bar{\mathbf{h}}^2 - \mathbf{h}^2}{(\phi_0/\xi^2)^2 |d_0|^4} + \frac{D_4[d_c, s_c]}{2\eta_0^4 |d_0|^4}}, \quad (4.1)$$

with  $F_0 = N_F \xi^2 \eta_0^2 \ln(T_c/T)$  and the magnetic flux density

$$\mathbf{B} = \overline{\mathbf{H}(\mathbf{r})} = \mathbf{H}_0 + \overline{\mathbf{h}(\mathbf{r})}. \quad (4.2)$$

Here, we write  $\int(\dots)d\mathbf{r}/\xi^2 = \overline{(\dots)}$ . In Eq. (4.1),  $D_4[d_c, s_c]$  is given by

$$\frac{D_4[d_c, s_c]}{|d_0|^4} = \frac{2}{3} \langle \phi_d^4 \rangle \frac{\overline{|d|^4}}{|d_0|^4} - \gamma \frac{\langle \phi_d^4 \hat{v}_+ \hat{v}_- \rangle}{3 \langle \phi_d^2 \hat{v}_+ \hat{v}_- \rangle} \left( 5 \overline{|\psi_0|^4} - 2 \overline{|\psi_1|^2 |\psi_0|^2} \right) + O(\gamma^2) \quad (4.3)$$

with

$$\frac{\overline{|d|^4}}{|d_0|^4} = \overline{|\psi_0|^4} + 4\gamma \text{Re} \left\{ \frac{d_4^{(1)}}{d_0} \overline{\psi_4 \psi_0^* |\psi_0|^2} \right\} + O(\gamma^2). \quad (4.4)$$

When a magnetic field has only the  $z$  component as in the present case, Eq. (4.1) is reduced to

$$\frac{F}{F_0} = \kappa^2 \frac{B^2}{(\phi_0/\xi^2)^2} - \frac{(B - H_{c2})^2}{(\phi_0/\xi^2)^2} \left\{ 1 + \frac{2\bar{\kappa}^2 C(a_y/a_x, \zeta, \theta_0)}{(\bar{h}_z/h_z^{(0)})^2} \right\}^{-1}, \quad (4.5)$$

where we use the notations

$$C(a_y/a_x, \zeta, \theta_0) \equiv \frac{D_4[d_c, s_c]}{|d_0|^4} - \frac{1}{2\bar{\kappa}^2} \frac{\bar{h}_z^2}{(h_z^{(0)})^2}, \quad (4.6)$$

$$\bar{\kappa} \equiv \phi_0 |d_0|^2 \left( 2\kappa h_z^{(0)} \xi^2 \eta_0^2 \right)^{-1} = \left( 2\sqrt{6} \langle \phi_d^2 \hat{v}_+ \hat{v}_- \rangle \right)^{-1} \frac{T}{T_c} \kappa_{\text{GL}}. \quad (4.7)$$

By using Eq. (3.29) and the orthogonalized condition  $\overline{\psi_{n_1} \psi_{n_2}^*} = \delta_{n_1, n_2}$ , the quantities  $\bar{h}_z$  in Eq. (4.5) and  $\bar{h}_z^2$  in Eq. (4.6) are given as follows,

$$\frac{\bar{h}_z}{h_z^{(0)}} = 1 + \gamma \left\{ \frac{(h_z^{(1)})_{0,0}}{h_z^{(0)}} + \frac{(h_z^{(1)})_{1,1}}{h_z^{(0)}} \right\} + O(\gamma^2), \quad (4.8)$$

$$\frac{\bar{h}_z^2}{(h_z^{(0)})^2} = \left\{ 1 + 2\gamma \frac{(h_z^{(1)})_{0,0}}{h_z^{(0)}} \right\} \overline{|\psi_0|^4} + 2\gamma \frac{(h_z^{(1)})_{1,1}}{h_z^{(0)}} \overline{|\psi_0|^2 |\psi_1|^2} + 4\gamma \text{Re} \left\{ \frac{(h_z^{(1)})_{4,0}}{h_z^{(0)}} \overline{\psi_4 \psi_0^* |\psi_0|^2} \right\} + O(\gamma^2). \quad (4.9)$$

In Eq. (4.5),  $2\bar{\kappa}^2 (\bar{h}_z/h_z^{(0)})^{-2} C(a_y/a_x, \zeta, \theta_0)$  corresponds to  $(2\kappa^2 - 1)\beta_A$  of the Abrikosov's theory.<sup>17</sup> In the limit  $\gamma \rightarrow 0$ , Eq. (4.5) is reduced to his result.

The quantities  $\overline{|\psi_0|^4}$ ,  $\overline{\psi_4 \psi_0^* |\psi_0|^2}$  and  $\overline{|\psi_1|^2 |\psi_0|^2}$  are calculated as follows from Eq. (2.12),

$$\overline{|\psi_0|^4} = \left( \frac{a_y}{a_x} \right)^{1/2} \sum_{n,m} \exp \left\{ -\pi \frac{a_y}{a_x} (m^2 + n^2) \right\} \cos(2\pi \zeta mn), \quad (4.10)$$

$$\begin{aligned} \overline{\psi_4 \psi_0^* |\psi_0|^2} &= \frac{1}{2\sqrt{6}} \left( \frac{a_y}{a_x} \right)^{1/2} \sum_{n,m} \left\{ \frac{3}{4} - 3(m-n)^2 \pi \frac{a_y}{a_x} + (m-n)^4 \left( \pi \frac{a_y}{a_x} \right)^2 \right\} \\ &\times \exp \left\{ -\pi \frac{a_y}{a_x} (m^2 + n^2) + i2\pi \zeta mn \right\}, \end{aligned} \quad (4.11)$$

$$\overline{|\psi_1|^2 |\psi_0|^2} = \frac{1}{2} \overline{|\psi_0|^4}. \quad (4.12)$$

These quantities depend on the parameters  $a_y/a_x$  and  $\zeta$  characterizing the unit cell shape of the vortex lattice. Therefore, the free energy (4.5) depends on the unit cell shape of the vortex lattice through the quantities  $\overline{|\psi_0|^4}$ ,  $\overline{\psi_4 \psi_0^* |\psi_0|^2}$  and  $\overline{|\psi_1|^2 |\psi_0|^2}$ . For the triangular lattice case ( $a_y/a_x = \sqrt{3}/2$ ,  $\zeta = 0.5$ ),  $\overline{\psi_4 \psi_0^* |\psi_0|^2} = 0$ . On the other hand, the orientation  $\theta_0$  of the vortex lattice affects the free energy (4.5) through  $d_4^{(1)}$  in Eq. (2.23) and  $(h_z^{(1)})_{4,0}$  in Eq. (3.28) as is seen from Eq. (2.27). Since  $\overline{h_z}$  does not depend on the orientation and the unit cell shape, the free energy (4.5) has its minimum at the vortex lattice structure where  $C(a_y/a_x, \zeta, \theta_0)$  defined in Eq. (4.6) takes a minimum value.

From Eqs. (4.3), (4.9) and (4.12),  $C(a_y/a_x, \zeta, \theta_0)$  is written as

$$\begin{aligned} C(a_y/a_x, \zeta, \theta_0) &= \left[ \frac{2}{3} \langle \phi_d^4 \rangle - \gamma \frac{4 \langle \phi_d^4 \hat{v}_+ \hat{v}_- \rangle}{3 \langle \phi_d^2 \hat{v}_+ \hat{v}_- \rangle} - \frac{1}{2\bar{\kappa}^2} \left\{ 1 - \gamma \left( \frac{11 \langle \phi_d^2 \hat{v}_+ \hat{v}_-^2 \rangle}{2 \langle \phi_d^2 \hat{v}_+ \hat{v}_- \rangle^2} + 7c_s \frac{\langle \phi_s \phi_d \hat{v}_+^2 \rangle \langle \phi_s \phi_d \hat{v}_-^2 \rangle}{\langle \phi_d^2 \hat{v}_+ \hat{v}_- \rangle^2} \right) \right\} \right] \overline{|\psi_0|^4} \\ &+ \frac{\sqrt{6}}{2} \left( \frac{2}{3} \langle \phi_d^4 \rangle - \frac{1}{2\bar{\kappa}^2} \right) \gamma \text{Re} \left\{ \left( \frac{\langle \phi_d^2 \hat{v}_-^4 \rangle}{\langle \phi_d^2 \hat{v}_+ \hat{v}_- \rangle^2} + 2c_s \frac{\langle \phi_s \phi_d \hat{v}_-^2 \rangle^2}{\langle \phi_d^2 \hat{v}_+ \hat{v}_- \rangle^2} \right) \overline{\psi_4 \psi_0^* |\psi_0|^2} \right\} + O(\gamma^2). \end{aligned} \quad (4.13)$$

When we use the  $\theta$ -integrated values in Eq. (2.27), Eq. (4.13) is reduced to

$$\begin{aligned} C(a_y/a_x, \zeta, \theta_0) &= \left[ 1 - 2\gamma - \frac{1}{2\bar{\kappa}^2} \left\{ 1 - \frac{1}{2} \gamma (11 + 7c_s) \right\} \right] \overline{|\psi_0|^4} \\ &+ \frac{\sqrt{6}}{4} \left( 1 - \frac{1}{2\bar{\kappa}^2} \right) \gamma (1 + 2c_s) \text{Re} \left\{ e^{-4i\theta_0} \overline{\psi_4 \psi_0^* |\psi_0|^2} \right\} + O(\gamma^2). \end{aligned} \quad (4.14)$$

The orientation of the vortex lattice is easily determined from Eq. (4.14). With respect to  $\theta_0$ , the minimum of  $C(a_y/a_x, \zeta, \theta_0)$  occurs at

$$\theta_0 = \frac{1}{4} \left\{ \arg \left( \overline{\psi_4 \psi_0^* |\psi_0|^2} \right) - \pi \right\}, \quad (4.15)$$

for  $c_s > -0.5$ , where  $\arg(\overline{\psi_4 \psi_0^* |\psi_0|^2})$  means the phase of the complex function  $\overline{\psi_4 \psi_0^* |\psi_0|^2}$ . Here,  $\bar{\kappa} \gg 1$  since we consider the case of an extreme type II superconductor. For  $c_s < -0.5$ , where  $V_s$  is strong repulsive, the minimum occurs at

$$\theta_0 = \frac{1}{4} \arg \left( \overline{\psi_4 \psi_0^* |\psi_0|^2} \right). \quad (4.16)$$

Then, the orientation  $\theta_0$  is rotated by  $\pi/4$  from that of the case  $c_s > -0.5$ . For both cases of Eqs. (4.15) and (4.16), the minimum of  $C(a_y/a_x, \zeta, \theta_0)$  as a function of  $\theta_0$  is given by

$$\begin{aligned} \bar{C}(a_y/a_x, \zeta) &\equiv \min_{\theta_0} \{ C(a_y/a_x, \zeta, \theta_0) \} \\ &= \left[ 1 - 2\gamma - \frac{1}{2\bar{\kappa}^2} \left\{ 1 - \frac{1}{2} \gamma (11 + 7c_s) \right\} \right] \overline{|\psi_0|^4} - \frac{\sqrt{6}}{4} \left( 1 - \frac{1}{2\bar{\kappa}^2} \right) \gamma |1 + 2c_s| \overline{|\psi_4 \psi_0^* |\psi_0|^2}|} + O(\gamma^2). \end{aligned} \quad (4.17)$$

We numerically estimate the minimum of  $\bar{C}(a_y/a_x, \zeta)$  with respect to  $a_y/a_x$  and  $\zeta$ . The term of  $\overline{|\psi_0|^4}$  prefers a triangular lattice, which is the well-known result in the conventional GL theory.<sup>17</sup> Then, at  $T = T_c$  (i.e.,  $\gamma = 0$ ), triangular lattice is realized as the equilibrium vortex lattice. On the other hand, the term of  $-\overline{|\psi_4 \psi_0^* |\psi_0|^2}|}$  prefers a square lattice. On lowering temperature from  $T_c$  (i.e., increasing  $\gamma$ ) along the curve of  $H_{c2}(T)$ , the contribution of  $-\overline{|\psi_4 \psi_0^* |\psi_0|^2}|}$  term increases. Then, the vortex lattice is deformed from a triangular lattice to a square lattice. There are three processes for this deformation, which are enumerated as (a), (b) and (c) in the following.

(a) On lowering temperature from  $T_c$ , the ratio  $a_y/a_x$  gradually varies from  $\sqrt{3}/2 = 0.866$  (triangular lattice) to 0.5 (square lattice) with preserving  $\zeta = 0.5$ . It means that the vortices form a shape of an isosceles triangle with  $BO = BA$  as schematically presented in Fig. 4. Since the function  $\overline{\psi_4\psi_0^*|\psi_0|^2}$  in Eq. (4.11) is real and negative in this case, the orientation is given by  $\theta_0 = 0$  for  $c_s > -0.5$ . (In the following, our calculation is restricted in the case  $c_s > -0.5$ .) Therefore, the base  $OA$  of the isosceles triangle is along the  $a$  axis direction.

(b) On lowering temperature from  $T_c$ , the parameters  $(a_y/a_x, \zeta)$  gradually vary from  $(\sqrt{3}/2, 0.5)$  [triangular lattice] to  $(1, 0)$  [square lattice] with keeping the shape of an isosceles triangle with  $OA = OB$ . In this process,  $\theta_0$  varies from  $30^\circ$  to  $45^\circ$  so that the base  $AB$  of the isosceles triangle is along the  $b$  direction.

(c) On lowering temperature from  $T_c$ , the parameters  $(a_y/a_x, \zeta)$  gradually vary from  $(\sqrt{3}/2, 0.5)$  to  $(1, 1)$  [square lattice] with keeping the shape of an isosceles triangle with  $AB = AO$ . In this process,  $\theta_0$  varies from  $-30^\circ$  to  $-45^\circ$  so that the base  $BO$  of an isosceles triangle is along the  $b$  direction.

The cases (b) and (c) are related each other by the relation  $C(a_y/a_x, 1 - \zeta, -\theta_0) = C(a_y/a_x, \zeta, \theta_0)$ . As a result, the cases (a), (b) and (c) are equivalent and give the same orientation and unit cell shape. The vortex lattice is deformed from a triangular lattice to a square lattice with keeping the shape of an isosceles triangle on lowering temperature from  $T_c$ . As for the orientation of the vortex lattice, the base of the isosceles triangle is along the  $a$  axis or the  $b$  axis direction. Therefore, at the lower temperature region, the equilibrium state of the vortex lattice is a square lattice tilted by  $\pi/4$  from the  $a$  axis, which is consistent with the result of Won and Maki<sup>23</sup>

To see the temperature dependence of the unit cell shape, we consider the case (a) in the limit  $\bar{\kappa} \gg 1$ . In this limit, Eq. (4.17) is reduced to

$$\bar{C}(a_y/a_x, \zeta) = (1 - 2\gamma)\overline{|\psi_0|^4} - \frac{\sqrt{6}}{4}\gamma|1 + 2c_s\overline{|\psi_4\psi_0^*|\psi_0|^2}| + O(\gamma^2), \quad (4.18)$$

where it is enough to consider only the contribution of the condensation energy. The ratio  $a_y/a_x$  in the equilibrium vortex lattice structure is evaluated from the minimum of  $\bar{C}(a_y/a_x, \zeta = 0.5)$  in Eq. (4.18). In Fig. 5, we present the temperature dependence of the ratio  $a_y/a_x$  along the curve of  $H_{c2}(T)$  for various mixing of the  $s$ -wave component,  $c_s = -0.2, -0.1, 0, 0.2, 0.4$ . As shown in Fig. 5, the deformation from a triangular lattice starts just below  $T_c$  on lowering temperature. In the pure  $d_{x^2-y^2}$ -wave case ( $c_s = 0$ ), the square lattice is realized for  $T \leq 0.858T_c$ . In the case  $V_s$  is attractive ( $c_s > 0$ ), the square lattice is realized from higher temperatures ( $T \leq 0.888T_c$  for  $c_s = 0.2$ ,  $T \leq 0.908T_c$  for  $c_s = 0.4$ ), since the contribution of  $-\overline{|\psi_4\psi_0^*|\psi_0|^2}$  in Eq. (4.18) is enhanced due to the induced  $s$ -wave order parameter. On the other hand, in the case  $V_s$  is repulsive ( $c_s < 0$ ), the temperature region of the square lattice is suppressed ( $T \leq 0.837T_c$  for  $c_s = -0.1$ ,  $T \leq 0.807T_c$  for  $c_s = -0.2$ ).

When we consider the case of an isotropic  $s$ -wave superconductor without the  $s$ - $d$  mixing ( $\phi_s \leftrightarrow \phi_d$ ,  $c_s = 0$  in Eq. (4.13)), by using Eq. (2.31) we obtain

$$C(a_y/a_x, \zeta, \theta_0) = \left\{ \frac{2}{3}(1 - 2\gamma) - \frac{1}{2\bar{\kappa}^2} \left( 1 - \frac{11}{2}\gamma \right) \right\} \overline{|\psi_0|^4} + O(\gamma^2). \quad (4.19)$$

In this isotropic  $s$ -wave case, the contribution of  $\overline{|\psi_4\psi_0^*|\psi_0|^2}$  is absent from  $C(a_y/a_x, \zeta, \theta_0)$ . Then, the minimum of  $\overline{|\psi_0|^4}$  determines the equilibrium vortex lattice structure. A triangular lattice is, therefore, realized in all the temperature region. It is consistent with the well-known result in the conventional GL theory.<sup>17</sup>

In the calculation of Won and Maki,<sup>23,24</sup> they obtain the equilibrium state by estimating the Abrikosov parameter  $\beta_A = \langle |\Delta(\mathbf{r}, \theta)|^4 \rangle / (\langle |\Delta(\mathbf{r}, \theta)|^2 \rangle)^2$ . It seems to be an analogy of the conventional GL theory. Within the order  $O(\gamma)$ , we obtain

$$\beta_A = \overline{|d|^4}/|d_0|^4 + O(\gamma^2) = \overline{|\psi_0|^4} - \frac{\sqrt{6}}{4}\gamma(1 + 2c_s)\text{Re}\{e^{-4i\theta_0}\overline{|\psi_4\psi_0^*|\psi_0|^2}\} + O(\gamma^2). \quad (4.20)$$

where it is noted that  $1 - 2\gamma$  in the first term of Eq. (4.14) is changed to 1. However,  $\beta_A$  itself should be modified by the correction of the order  $O(\gamma)$ . In our calculation, we use the function  $C(a_y/a_x, \zeta, \theta_0)$  in Eq. (4.14) instead of  $\beta_A$ . It changes the result quantitatively. Dominant terms neglected in the estimate by  $\beta_A$  come from the gradient term of the  $\Delta^3$ -order such as  $\langle \phi_d^4(\hat{\mathbf{v}} \cdot \hat{\mathbf{q}})^2 d \rangle |d|^2$  in the GL equation. If we consider the correction of the non-local term  $\langle \phi_d^2(\hat{\mathbf{v}} \cdot \hat{\mathbf{q}})^4 d \rangle$  in the calculation of the  $\Delta$ -linear order, in the estimate of the free energy we have to include also the gradient terms of the  $\Delta^3$ -order as correction, which appear within the same order of  $\gamma$ .

While Won and Maki considered only the cases of a triangular lattice and a square lattice, they obtain the result that the square lattice is stabilized at  $T < 0.88T_c$  in the pure  $d_{x^2-y^2}$ -case. This temperature is not so different from ours. In their result, as repulsion of the  $s$ -wave component increases in the interaction, the temperature region of the

square lattice is suppressed (Fig. 4 of Ref. 23). This tendency of the repulsive case is consistent with our result. Won and Maki<sup>23,24</sup> suggested that the experimental result of an oblique lattice<sup>2-4</sup> can be explained by the square lattice structure obtained here and by the scaling of the coordinate system due to the difference of the coherence lengths between the  $a$  axis and the  $b$  axis.

## V. SPATIAL VARIATION OF THE VORTEX LATTICE STRUCTURE IN THE PURE $D_{x^2-y^2}$ -WAVE CASE

As clarified in previous sections, the characteristic features of the  $d_{x^2-y^2}$ -wave superconductor's vortex lattice is produced by the appearance of the fourth Landau level function  $\psi_4(\mathbf{r}|\mathbf{r}_0)$  in the vortex lattice structure. Due to this effect, the vortex lattice is deformed from a triangular lattice to a square lattice as shown in Sec. IV. In this section, we consider the effect of  $\psi_4(\mathbf{r}|\mathbf{r}_0)$  on the spatial variation of the vortex lattice structure in a  $d_{x^2-y^2}$ -wave superconductor by using the results of Secs. II and III. Here, we consider the case of the pure  $d_{x^2-y^2}$ -wave superconductor ( $c_s = 0$ ). Then, in the following characteristic features of the vortex lattice, there is no contribution of the induced  $s$ -wave order parameter.

First, we consider the spatial variation of the  $d_{x^2-y^2}$ -wave order parameter, which is given by Eq. (2.29). The contour plot of the amplitude,  $|d(\mathbf{r})/d_0|$ , is presented in Fig. 6, where the core region of the vortex is darkly shaded. We consider the case of a square lattice at a lower temperature [Figs. 6 (a) and (b)] and the case of an oblique lattice at an intermediate temperature [Fig. 6 (c)]. The parameter  $\gamma$  is chosen by following the result of Fig. 5.

As for the case of a square lattice ( $a_y/a_x=0.5$ ,  $\zeta=0.5$ ), we use  $\gamma=0.2$  ( $T/T_c=0.802$ ). In addition to the case of an equilibrium orientation  $\theta_0 = 0^\circ$  in Fig. 6 (a), we also show the case of an unstable orientation  $\theta_0 = 45^\circ$  in Fig. 6 (b) to clarify the contribution of  $\psi_4(\mathbf{r}|\mathbf{r}_0)$ . In both figures, the  $a$  axis and the  $b$  axis are along the horizontal and vertical directions. (In Fig. 6 (a), the  $x$  axis and the  $y$  axis are also along the horizontal and vertical directions. In Fig. 6 (b), the  $x$  axis and the  $y$  axis are rotated by  $45^\circ$  from the case of Fig. 6 (a).) Due to the property of a  $d_{x^2-y^2}$ -wave superconductor, the amplitude of the order parameter is slightly suppressed along the direction of the  $a$  axis and the  $b$  axis around a vortex, which has been exhibited in the calculation of the single vortex case.<sup>18,19</sup> On the other hand, due to the property of the vortex lattice, the amplitude of the order parameter is slightly suppressed along the directions of nearest-neighbor vortices, which has been exhibited in the calculation of the isotropic  $s$ -wave superconductor case.<sup>25</sup> Therefore, when the  $a$  axis and the  $b$  axis agree with the nearest neighbor directions as in the case of Fig. 6 (b), the suppression along the nearest neighbor directions is enhanced and the fourfold symmetric vortex core structure is emphasized. On the other hand, when the  $a$  axis and the  $b$  axis are away from the nearest-neighbor directions as in the case of Fig. 6 (a), the suppression of both effects cancels each other. Therefore, the vortex core structure is reduced to a cylindrically symmetric one. It seems that the gain of the condensation energy in the case of Fig. 6 (a) is more efficient than that of Fig. 6 (b). Then, the equilibrium vortex lattice structure prefers the configuration of Fig. 6 (a).

Figure 6 (c) is the case of an oblique lattice with  $73^\circ$  ( $a_y/a_x=0.676$ ,  $\zeta=0.5$ ) for the equilibrium orientation  $\theta_0 = 0$ , where we use  $\gamma=0.115$  ( $T/T_c=0.881$ ). In this figure, the  $a$  axis and the  $b$  axis (and the  $x$  axis and the  $y$  axis) are along the horizontal and vertical directions. Also in this oblique lattice case for  $\theta_0 = 0$ , the vortex core has cylindrically symmetric structure since the  $a$  axis and the  $b$  axis are away from the nearest-neighbor directions.

Next, we consider the spatial variation of the current and the induced magnetic field around vortices in each case of Fig. 6. The current is calculated from Eqs. (3.15) and (3.16), where we use the  $\theta$ -integrated values of Eq. (2.27). Figure 7 shows the contour plot for the amplitude of the current,  $|\mathbf{j}(\mathbf{r})|/(\pi\sqrt{\epsilon\xi^2}/2\kappa^2\eta^2)$ . The corresponding magnetic field is calculated from Eq. (3.30). Figure 8 shows the contour plot of the magnetic field,  $h_z(\mathbf{r})/|h_z^{(0)}|$ . The contour lines are also interpreted as the stream lines of the current.

The calculation of the single vortex lattice case shows that  $|\mathbf{j}(\mathbf{r})|$  and  $h_z(\mathbf{r})$  are fourfold symmetric around a vortex core in a  $d_{x^2-y^2}$ -wave superconductor.<sup>18,19</sup> There,  $|\mathbf{j}(\mathbf{r})|$  has four peaks around the vortex core at the direction of  $45^\circ$  from the  $a$  axis or the  $b$  axis. Reflecting this current distribution, the magnetic field extends along the  $a$  axis and the  $b$  axis directions around the vortex core. This is because the field is strongly screened by the induced current along the  $45^\circ$  directions. These fourfold symmetric structures of  $|\mathbf{j}(\mathbf{r})|$  and  $h_z(\mathbf{r})$  are also recognized in our calculation of the vortex lattice case, which becomes clear with increasing  $\gamma$  (lowering temperature).

In the square lattice case at a lower temperature ( $\gamma = 0.2$ ), we compare the case of the equilibrium orientation  $\theta_0 = 0^\circ$  in Figs. 7 (a) and 8 (a) with that of the unstable orientation  $\theta_0 = 45^\circ$  in Figs. 7 (b) and 8 (b). For the equilibrium case  $\theta_0 = 0^\circ$ , the screening current flows in the narrow region around each vortex compared with the unstable case  $\theta_0 = 45^\circ$ . Then, for  $\theta_0 = 0^\circ$ , the enhancement of  $h_z(\mathbf{r})$  at each vortex core localizes in the narrow region, and  $h_z(\mathbf{r})$  is reduced to be a flat distribution at the region apart from vortex cores.

Figure 7 (c) and 8 (c) are the oblique lattice case at the intermediate temperature ( $\gamma = 0.115$ ). There, fourfold symmetric structure of  $|\mathbf{j}(\mathbf{r})|$  and  $h_z(\mathbf{r})$  are not seen so clearly due to the small  $\gamma$  and also due to the broken fourfold symmetry of the vortex lattice structure.

Another way to investigate the spatial variation of  $h_z(\mathbf{r})$  is to consider the magnetic field distribution function defined as

$$P(h) = \int_{\text{unit cell}} \delta(h - h_z(\mathbf{r})) d\mathbf{r} / a_x a_y, \quad (5.1)$$

which is related to the resonance line shape in the  $\mu$ SR and NMR experiments. In Fig. 9, we show  $P(h)$  as a function of  $h/|h_z^{(0)}|$  for the equilibrium state of the vortex lattice at various temperatures;  $\gamma = 0$  (a), 0.06 (b), 0.115 (c), 0.15 (d) and 0.2 (e), which correspond to  $T/T_c = 1, 0.936, 0.881, 0.848$  and  $0.802$ , respectively. The case of a pure  $d_{x^2-y^2}$ -wave superconductor given by Eq. (3.30) is presented by solid lines. The parameters of the vortex lattice are chosen by following the result of Fig. 5. Then,  $\zeta = 0.5$ ,  $\theta_0 = 0$  and  $a_y/a_x = 0.866$  (a), 0.799 (b), 0.676 (c), 0.5 (d), 0.5 (e). In the case of a triangular lattice [line (a)] and a square lattice [lines (d) and (e)],  $P(h)$  has single peak structure. On the other hand, in the case of an oblique lattice [lines (b) and (c)],  $P(h)$  has double peaks structure. These structures are consistent with the result of Franz *et al.*,<sup>8,9</sup> while the oblique lattice is derived from the induced  $s$ -wave order parameter in their theory. As explained by them, the double peak structure occurs in an oblique lattice because the saddle points of  $h_z(\mathbf{r})$  between two vortices are not equivalent in the  $\mathbf{r}_1$  direction and in the  $\mathbf{r}_2$  direction.

For comparison, we also show  $P(h)$  of the isotropic  $s$ -wave case given by Eq. (3.31), which is presented by dotted lines in Fig. 9. In this  $s$ -wave case, the equilibrium state is a triangular lattice ( $\zeta = 0.5$ ,  $a_y/a_x = 0.866$ ). We compare the case of a square lattice in a pure  $d_{x^2-y^2}$ -wave superconductor with that of a triangular lattice in a isotropic  $s$ -wave superconductor. At  $\gamma = 0.16$  [line (d)], the peak of the square lattice case locates at the right side of the peak of the triangular lattice case, which is consistent with the result of the conventional GL theory.<sup>26</sup> In the  $d_{x^2-y^2}$ -wave case, with increasing  $\gamma$  (decreasing  $T$ ), the lower edge of  $P(h)$  approaches the peak position and the peak height increases as is seen from the line (e). This change of the distribution reflects the result of Fig. 8 (a), where  $h_z(\mathbf{r})$  has uniform distribution outside the core region. In the isotropic  $s$ -wave case, on the other hand, the distribution of  $P(h)$  does not so vary on lowering temperature.

Some of the above-mentioned features are similar to that of Berlinsky *et al.*,<sup>7-9</sup> where the characteristic features of the vortex lattice are derived from the contribution of the induced  $s$ -wave order parameter. However, it is important to notice that the characteristic features suggested by our calculation occur even in the pure  $d_{x^2-y^2}$ -wave case where the induced  $s$ -wave order parameter is absent. Its origin is the  $A_4$ -terms in Eq. (2.4), which is in the order  $O(\ln(T_c/T))$  in the dimensionless form of the GL equation and neglected in the conventional GL equation. The contribution of these correction terms increases with lowering temperature from  $T_c$  and leads to the fourfold symmetric vortex core structure. It also induces the  $\psi_4(\mathbf{r}|\mathbf{r}_0)$  term in the vortex lattice structure and leads to the above-mentioned characteristic features of the vortex lattice in a  $d_{x^2-y^2}$ -wave superconductor.

If the induced  $s$ -wave order parameter cannot be neglected, the contribution of the  $\psi_4(\mathbf{r}|\mathbf{r}_0)$  term increases for  $c_s > 0$  and decreases for  $c_s < 0$ , as shown in the result of Secs. II and III. Therefore, the above-mentioned characteristic features, which are produced by the  $\psi_4(\mathbf{r}|\mathbf{r}_0)$  term, are enhanced in the case  $V_s$  is attractive ( $c_s > 0$ ) and suppressed in the case  $V_s$  is repulsive ( $c_s < 0$ ).

## VI. SUMMARY AND DISCUSSIONS

We investigate the vortex lattice structure in a  $d_{x^2-y^2}$ -wave superconductor near  $H_{c2}$  in the framework of the extended GL theory. We determine the orientation and the unit cell shape of the vortex lattice. As for the unit cell shape, vortices form a shape of an isosceles triangle as shown in Fig. 4. The vertical angle gradually varies from  $60^\circ$  to  $90^\circ$  when temperature is lowered from  $T_c$ . Then, a square lattice is realized at the low temperature region  $T < 0.86T_c$  for the pure  $d_{x^2-y^2}$ -wave case ( $c_s = 0$ ). As for the orientation, the base of an isosceles triangle is along the  $a$  axis (or the  $b$  axis).

We also calculate the spatial variation of the vortex structure, such as the  $d_{x^2-y^2}$ -wave order parameter, the current and the induced magnetic field. As temperature is enough lowered, the fourfold symmetric core structure clearly appears in our calculation of the vortex lattice case. This structure is consistent with that of the single vortex case. The amplitude of the current has four peaks around each vortex in the  $45^\circ$  direction from the  $a$  axis. Then, the induced magnetic field extends along the  $a$  axis and the  $b$  axis direction. As for the  $d_{x^2-y^2}$ -wave order parameter, the amplitude around the vortex is slightly suppressed along the  $a$  axis and the  $b$  axis direction due to the nature of the  $d_{x^2-y^2}$ -wave superconductivity. On the other hand, the amplitude is slightly suppressed in the direction of the nearest-neighbor vortex. When the  $a$  axis and the  $b$  axis are away from the nearest-neighbor directions (i.e., the case

of the orientation  $\theta_0 = 0^\circ$ ), the suppression of both effects cancels each other. Therefore, the vortex core structure is reduced to a cylindrically symmetric one. This structure seems to most effectively gain the condensation energy. It is the reason why the equilibrium state prefers the orientation  $\theta_0 = 0^\circ$ .

Some of the above-mentioned characteristic features of the vortex lattice are similar to that of Berlinsky *et al.*,<sup>7-9</sup> where the origin of the characteristic features in their result is the mixing of the induced  $s$ -wave order parameter. However, it is noted that the characteristic features obtained in this paper appear even in the pure  $d_{x^2-y^2}$ -wave case where the induced  $s$ -wave order parameter is absent. The origin of these characteristic features is the higher order terms of the order parameter and the higher derivatives (or non-local terms) which are neglected in the conventional GL theory. These correction terms derived from the Gor'kov equation are higher order in the small parameter  $\ln(T_c/T)$ . Therefore, their contribution vanishes at  $T_c$ , but becomes increasingly important upon lowering temperature from  $T_c$ . Some of these correction terms induce the contribution of the fourth Landau level function  $\psi_4(\mathbf{r}|\mathbf{r}_0)$  to the vortex lattice structure within the order  $O(\ln(T_c/T))$ . This contribution of  $\psi_4(\mathbf{r}|\mathbf{r}_0)$  leads to the characteristic features of the vortex lattice in the  $d_{x^2-y^2}$ -wave superconductor, such as the deformation from a triangular lattice and the fourfold symmetric structure around a vortex core.

We also estimate the effect of the induced  $s$ -wave order parameter. The amplitude of the  $s$ -wave order parameter depends on  $V_s$ , the  $s$ -wave component of the pairing interaction, through the parameter  $c_s$  defined in Eq. (2.8) in our model. When the contribution of the induced  $s$ -wave order parameter cannot be neglected, the factor of the  $\psi_4(\mathbf{r}|\mathbf{r}_0)$  term increases (decreases) for  $c_s > 0$  ( $c_s < 0$ ) in the expression of the vortex lattice structure. Then, the characteristic features, which is produced by the  $\psi_4(\mathbf{r}|\mathbf{r}_0)$  term, are enhanced (suppressed) in the case  $V_s$  is attractive (repulsive).

In the following, we give some comments.

At further low temperatures, we have to consider further higher order derivatives in the GL equation. Then, the contribution of higher Landau level functions  $\psi_8(\mathbf{r}|\mathbf{r}_0)$ ,  $\psi_{12}(\mathbf{r}|\mathbf{r}_0)$ ,  $\dots$ , appear in the vortex lattice structure, which are in the order  $O([\ln(T_c/T)]^n)$  ( $n \geq 2$ ). The investigation of these higher order correction is now in progress.

The fourfold symmetric behavior is also observed when magnetic field is applied in the direction parallel to the  $ab$  plane. When the direction of the field is rotated within the plane, the  $H_{c2}$  (Refs. 27 and 28) and the torque (Ref. 29) experiments show the fourfold symmetric behavior. They are explained by the contribution of the higher order derivative terms (or non-local terms) in the GL equation as in this paper.<sup>24,30,31</sup> Also in this parallel field case, if the induced  $s$ -wave order parameter exists, the fourfold symmetric behavior is enhanced (suppressed) when  $V_s$  is attractive (repulsive).<sup>32</sup>

The amplitude of the induced  $s$ -wave order parameter depends on  $V_s$ , the  $s$ -wave component of the interaction, through the parameter  $c_s$  in Eq. (2.8). Then, next, we want to know the value of  $V_s$  appropriate for the high- $T_c$  materials. However, it seems to be a difficult problem, which is deeply related to the pairing mechanism of the high- $T_c$  superconductors. If the  $s$ -wave order parameter is defined as the on-site pairing,  $V_s$  may be strongly repulsive since the high- $T_c$  materials are strongly correlated electron systems. However,  $s$ -wave order parameter is defined as the extended  $s$ -wave, we cannot exclude the possibility of the attractive  $V_s$ . The extended  $s$ -wave is derived from the non-local pairing between nearest neighbor atomic site, which is the same origin of the  $d_{x^2-y^2}$ -wave pairing.

We note that it is not clear whether the two-component GL theory can be applied to the case of strongly repulsive  $V_s$ . In the limit of strong repulsive  $V_s$  ( $c_s \rightarrow -\infty$ ), the induced  $s$ -wave order parameter completely destroys the  $d_{x^2-y^2}$ -wave superconductivity, which is seen from Eq. (2.32) for example. In this strong repulsive case, we have to reconsider from the outset whether we can introduce the  $s$ -wave order parameter or not.

So far, we consider the case of the isotropic Fermi surface. If the Fermi surface is anisotropic, the average  $\langle \dots \rangle$  is modified to  $\langle \dots \rho(\theta) \rangle$ , where  $\rho(\theta)$  is the  $\theta$ -dependent factor of the density of states on the Fermi surface and  $\int \rho(\theta) d\theta / 2\pi = 1$ . And  $|\hat{\mathbf{v}}|$  has the  $\theta$ -dependence.

The origin of the fourfold symmetric core structure and the deformation from a triangular lattice is the appearance of  $\psi_4(\mathbf{r}|\mathbf{r}_0)$  in the vortex lattice structure. The contribution of  $\psi_4(\mathbf{r}|\mathbf{r}_0)$  is proportional to the quantity  $\langle \phi_d^2 v_-^4 \rho \rangle$  in the pure  $d_{x^2-y^2}$ -wave case. Even in the  $s$ -wave superconductor ( $\phi_d \rightarrow \phi_s$ ), when the structure of the Fermi surface or the energy gap ( $|\phi_s|$ ) have the anisotropic component with fourfold symmetry, the contribution of  $\psi_4(\mathbf{r}|\mathbf{r}_0)$  appears since  $\langle \phi_s^2 v_-^4 \rho \rangle \neq 0$ . Then, the fourfold symmetric core structure and the deformation from a triangular lattice occur at lower temperature and higher magnetic field. The square lattice observed by De Wilde *et al.*<sup>33</sup> in the STM image of the vortex lattice on  $\text{LuNi}_2\text{B}_2\text{C}$  seems to be this case. And Eskildsen *et al.*<sup>34</sup> reported the deformation from a triangular lattice to a square lattice with increasing magnetic field by the SANS and magnetic decoration observation of the flux line lattice on  $\text{ErNi}_2\text{B}_2\text{C}$ , where the orientation and the unit cell shape of the vortex lattice in the deforming process agree with our results. In the  $d_{x^2-y^2}$ -wave superconductor,  $|\langle \phi_d^2 v_-^4 \rho \rangle|$  takes a large value since  $\phi_d^2$  has fourfold symmetric node structure. In the  $s$ -wave superconductor, to introduce a large value of  $|\langle \phi_s^2 v_-^4 \rho \rangle|$  comparable to the  $d_{x^2-y^2}$ -wave case,  $\phi_s^2 |v_-|^4 \rho$  should have a large anisotropy with fourfold symmetry such as the form of  $(1 + \cos 4\theta)/2$ .



## ACKNOWLEDGMENTS

We are grateful to K. Takanaka for informing us the detail of his calculation. We also would like to thank N. Hayashi and T. Sugiyama for fruitful discussions. One of the authors (M. I.) would like to thank the Japan Society for the Promotion of Science for financial support.

### APPENDIX A: FREE ENERGY OF THE VORTEX LATTICE STATE

The expression of the free energy  $F$  is determined so that  $\partial F/\partial d^*(\mathbf{r}) = 0$  and  $\partial F/\partial s^*(\mathbf{r}) = 0$ , respectively, give the GL equations (2.6) and (2.7). Thus, the free energy is written as

$$\begin{aligned} \frac{F}{F_0} &= \kappa^2 \frac{\overline{\mathbf{H}(\mathbf{r})^2}}{(\phi_0/\xi^2)^2} + \eta_0^{-2} \left\{ -\overline{|d|^2} + (c_s\gamma)^{-1}\overline{|s|^2} + \overline{d^*Kd} + \overline{s^*K_{ss}s} + \overline{s^*K_{sd}d} + \overline{d^*K_{sd}s} \right\} \\ &+ \frac{1}{2}\eta_0^{-4}D_4[d, s] + \frac{1}{3}\eta_0^{-6}\overline{d^*R_5} + O(\gamma^2) \end{aligned} \quad (\text{A1})$$

with

$$D_4[d, s] = \overline{d^*R_3} + \frac{2}{3}\langle\phi_s^4\rangle\overline{|s|^4} + \frac{2}{3}\langle\phi_s^2\phi_d^2\rangle \left( 4\overline{|s|^2|d|^2} + \overline{s^2d^{*2}} + \overline{d^2s^{*2}} \right), \quad (\text{A2})$$

where

$$R_3 = \frac{2}{3}\langle\phi_d^4\rangle|d|^2d - \frac{2}{3}\gamma\xi^2\langle\phi_d^4[4\{(\hat{\mathbf{v}} \cdot \mathbf{q})^2d\}|d|^2 + d^2\{(\hat{\mathbf{v}} \cdot \mathbf{q})^2d\}^* - 2d|(\hat{\mathbf{v}} \cdot \mathbf{q})d|^2 + 3\{(\hat{\mathbf{v}} \cdot \mathbf{q})d\}^2d^*]\rangle, \quad (\text{A3})$$

$$R_5 = -\frac{1}{3}\gamma\langle\phi_d^6\rangle|d|^4d, \quad (\text{A4})$$

$$K = 2\xi^2\langle\phi_d^2(\hat{\mathbf{v}} \cdot \mathbf{q})^2\rangle - 2\gamma\xi^4\langle\phi_d^2(\hat{\mathbf{v}} \cdot \mathbf{q})^4\rangle, \quad (\text{A5})$$

$$K_{ss} = 2\xi^2\langle\phi_s^2(\hat{\mathbf{v}} \cdot \mathbf{q})^2\rangle, \quad (\text{A6})$$

$$K_{sd} = 2\xi^2\langle\phi_s\phi_d(\hat{\mathbf{v}} \cdot \mathbf{q})^2\rangle. \quad (\text{A7})$$

From  $\partial F/\partial \mathbf{A}(\mathbf{r}) = 0$ , the expression of the current density is reproduced as follows,

$$\mathbf{j}(\mathbf{r}) = \xi\nabla \times \mathbf{h}(\mathbf{r})/(\phi_0/\xi^2) = -\frac{\phi_0}{2\kappa^2\xi} \left\{ \frac{1}{\eta_0^2} \left( d^* \frac{\partial K}{\partial \mathbf{A}} d + s^* \frac{\partial K_{ss}}{\partial \mathbf{A}} s + s^* \frac{\partial K_{sd}}{\partial \mathbf{A}} d + d^* \frac{\partial K_{ds}}{\partial \mathbf{A}} s \right) + \frac{1}{2\eta_0^4} d^* \frac{\partial R_3}{\partial \mathbf{A}} \right\}. \quad (\text{A8})$$

Equation (A8) is equivalent to Eq. (3.3), if we neglect the term of  $d^*(\partial R_3/\partial \mathbf{A})$  which is the order  $O(|d_0|^4)$ . From  $\overline{d^*(\partial F/\partial d^*)} = 0$  and  $\overline{s^*(\partial F/\partial s^*)} = 0$ , we obtain the following relations,

$$\eta_0^{-2}\overline{|d|^2} = \eta_0^{-2}(\overline{d^*Kd} + \overline{d^*K_{sd}s}) + \eta_0^{-4} \left\{ \overline{d^*R_3} + \frac{2}{3}\langle\phi_s^2\phi_d^2\rangle \left( 2\overline{|s|^2|d|^2} + \overline{s^2d^{*2}} \right) \right\} + \eta_0^{-6}\overline{d^*R_5}, \quad (\text{A9})$$

$$-\frac{\overline{|s|^2}}{c_s\gamma\eta_0^2} = \eta_0^{-2}(\overline{s^*K_{ss}s} + \overline{s^*K_{sd}d}) + \eta_0^{-4} \left\{ \frac{2}{3}\langle\phi_s^4\rangle\overline{|s|^4} + \frac{2}{3}\langle\phi_s^2\phi_d^2\rangle \left( 2\overline{|d|^2|s|^2} + \overline{d^2s^{*2}} \right) \right\}. \quad (\text{A10})$$

By substituting Eqs. (A9) and (A10) into Eq. (A1), the free energy is reduced to

$$\frac{F}{F_0} = \kappa^2 \frac{\overline{\mathbf{H}(\mathbf{r})^2}}{(\phi_0/\xi^2)^2} - \frac{1}{2}\eta_0^{-4}D_4[d, s] - \frac{2}{3}\eta_0^{-6}\overline{d^*R_5}. \quad (\text{A11})$$

By using the magnetic flux density  $\mathbf{B}$  in Eq. (4.2),

$$\mathbf{H}(\mathbf{r}) = \mathbf{H}_0 + \mathbf{h}(\mathbf{r}) = \mathbf{B} - \overline{\mathbf{h}(\mathbf{r})} + \mathbf{h}(\mathbf{r}). \quad (\text{A12})$$

Thus,  $\overline{\mathbf{H}(\mathbf{r})^2}$  in the first term of Eq. (A11) is written as

$$\overline{\mathbf{H}(\mathbf{r})^2} = \mathbf{B}^2 - \overline{\mathbf{h}}^2 + \overline{\mathbf{h}^2}. \quad (\text{A13})$$

We now consider the behavior in the immediate vicinity of  $H_{c2}$ . The quantities  $d(\mathbf{r})$ ,  $s(\mathbf{r})$ ,  $\mathbf{A}(\mathbf{r})$  and  $\mathbf{H}(\mathbf{r})$  are, respectively, divided into the values at  $H_{c2}$  (we denote them as  $d_c$ ,  $s_c$ ,  $\mathbf{A}_c$  and  $\mathbf{H}_{c2}$ ) and the deviations from them,

$$d = d_c + \delta d, \quad s = s_c + \delta s, \quad \mathbf{A} = \mathbf{A}_c + \delta \mathbf{A}, \quad (\text{A14})$$

$$\mathbf{H}(\mathbf{r}) = \mathbf{H}_{c2} + \{\mathbf{H}_0 - \mathbf{H}_{c2} + \mathbf{h}(\mathbf{r})\}, \quad (\text{A15})$$

where we have relations,

$$\nabla \times \mathbf{A}_c = \mathbf{H}_{c2}, \quad \nabla \times \delta \mathbf{A} = \mathbf{H}_0 - \mathbf{H}_{c2} + \mathbf{h}(\mathbf{r}). \quad (\text{A16})$$

By using Eq. (A14), the kernels  $K$ ,  $K_{ss}$  and  $K_{sd}$  are also divided into two parts, for example,

$$K(\mathbf{A}) = K^{(c)} + \frac{\partial K^{(c)}}{\partial \mathbf{A}} \cdot \delta \mathbf{A}, \quad (\text{A17})$$

where we write

$$K^{(c)} = K(\mathbf{A}_c), \quad \frac{\partial K^{(c)}}{\partial \mathbf{A}} = \left. \frac{\partial K}{\partial \mathbf{A}} \right|_{\mathbf{A}=\mathbf{A}_c}. \quad (\text{A18})$$

While the deviations  $\delta d/d_c$ ,  $\delta s/s_c$  and  $|\delta \mathbf{A}|/|\mathbf{A}_c|$  are in the order of small quantity  $(H_0 - H_{c2})/H_{c2}$ , the order parameters  $d_c$  and  $s_c$  themselves are also small quantities in the immediate vicinity of  $H_{c2}$ . The order parameters  $d_c$  and  $s_c$ , which have been already obtained in Sec. II, satisfy the linearized GL equations,

$$-d_c + K^{(c)}d_c + K_{sd}^{(c)}s_c = 0, \quad (\text{A19})$$

$$(c_s \gamma)^{-1}s_c + K_{ss}^{(c)}s_c + K_{sd}^{(c)}d_c = 0. \quad (\text{A20})$$

Equations (A19) and (A20) are equivalent to Eqs. (2.10) and (2.11), respectively. By substituting Eqs. (A14) and (A17), Eq. (A8) is reduced to

$$\mathbf{j}(\mathbf{r}) = \xi \nabla \times \mathbf{h}(\mathbf{r}) / (\phi_0 / \xi^2) = -\frac{\phi_0}{2\kappa^2 \eta_0^2 \xi} \left( d_c^* \frac{\partial K^{(c)}}{\partial \mathbf{A}} d_c + s_c^* \frac{\partial K_{ss}^{(c)}}{\partial \mathbf{A}} s_c + d_c^* \frac{\partial K_{sd}^{(c)}}{\partial \mathbf{A}} s_c + s_c^* \frac{\partial K_{sd}^{(c)}}{\partial \mathbf{A}} d_c \right) \quad (\text{A21})$$

within the order  $O(|d_0|^2)$ . In this order,  $\mathbf{j}(\mathbf{r})$  and  $\mathbf{h}(\mathbf{r})$  in Eq. (A21) are reduced to the ones obtained in Sec. III [Eqs. (3.15), (3.16) and (3.29)].

On the other hand, by substituting Eqs. (A14) and (A17) into Eqs. (A9) and (A10) and by using Eqs. (A19) and (A20), we obtain

$$\kappa^2 (\phi_0 / \xi^2)^{-2} \overline{(\nabla \times \mathbf{h}) \cdot \delta \mathbf{A}} = \frac{1}{2} \eta_0^{-4} D_4, \quad (\text{A22})$$

where  $\nabla \times \mathbf{h}$  comes from the relation of Eq. (A21). From Eqs. (A16) and (4.2), there is a relation

$$\overline{(\nabla \times \mathbf{h}) \cdot \delta \mathbf{A}} = \overline{(\nabla \times \delta \mathbf{A}) \cdot \mathbf{h}} = \overline{(\mathbf{H}_0 - \mathbf{H}_{c2} + \mathbf{h}) \cdot \mathbf{h}} = (\mathbf{B} - \mathbf{H}_{c2}) \cdot \overline{\mathbf{h}} - \overline{\mathbf{h}}^2 + \overline{\mathbf{h}^2}. \quad (\text{A23})$$

Thus, by using Eqs. (A22) and (A23), we obtain an identity

$$|d_0|^2 = \frac{\kappa^2 (\mathbf{B} - \mathbf{H}_{c2}) \cdot \overline{\mathbf{h}}}{(\phi_0 / \xi^2)^2 |d_0|^2} \frac{1}{\kappa^2 \frac{\overline{\mathbf{h}}^2 - \mathbf{h}^2}{(\phi_0 / \xi^2)^2 |d_0|^4} + \frac{D_4 [d_c, s_c]}{2\eta_0^4 |d_0|^4}}, \quad (\text{A24})$$

which determines the amplitude of the order parameter. Equation (A24) corresponds to the “first Abrikosov identity”.

By substituting Eqs. (A13), (A14) and (A17) into Eq. (A11), the free energy is written as

$$\frac{F}{F_0} = \kappa^2 \frac{\mathbf{B}^2}{(\phi_0/\xi^2)^2} - \left\{ \kappa^2 \frac{\bar{\mathbf{h}}^2 - \bar{\mathbf{h}}^2}{(\phi_0/\xi^2)^2 |d_0|^4} + \frac{D_4[d_c, s_c]}{2\eta_0^4 |d_0|^4} \right\} |d_0|^4 + O(|d_0|^6). \quad (\text{A25})$$

Equation (4.1) is obtained by the substitution of (A24) into Eq. (A25).

As for  $D_4$  defined in Eq. (A2), the terms except for  $\bar{d}R_3$  is in the order  $O(\gamma^2)$ , since  $s$  is in the order  $O(\gamma)$  as is seen from Eq. (2.26). Thus,  $D_4[d_c, s_c]$  of Eq. (4.4) is obtained by substituting Eqs. (2.9) and (2.25) into Eqs. (A2) and (A3).

- <sup>1</sup> *Anisotropy Effects in Superconductors*, edited by H. W. Weber (Plenum Press, New York, 1976).
- <sup>2</sup> B. Keimer, W. Y. Shih, R. W. Erwin, J. W. Lynn, F. Dogan, and I. A. Aksay, Phys. Rev. Lett. **73**, 3459 (1994).
- <sup>3</sup> I. Maggio-Aprile, Ch. Renner, A. Erb, E. Walker, and Ø. Fischer, Phys. Rev. Lett. **75**, 2754 (1995).
- <sup>4</sup> Ch. Renner, I. Maggio-Aprile, A. Erb, E. Walker, and Ø. Fischer, in *Spectroscopic Studies of Superconductors*, edited by I. Bozovic and D. van der Marel, Proc. SPIE **2696B**, 322 (1996).
- <sup>5</sup> M. B. Walker and T. Timusk, Phys. Rev. B **52**, 97 (1995).
- <sup>6</sup> G. J. Dolan, F. Holtzberg, C. Feild, and T. R. Dinger, Phys. Rev. Lett. **62**, 2184 (1989).
- <sup>7</sup> A. J. Berlinsky, A. L. Fetter, M. Franz, C. Kallin, and P. I. Soininen, Phys. Rev. Lett. **75**, 2200 (1995).
- <sup>8</sup> M. Franz, C. Kallin, P. I. Soininen, A. J. Berlinsky, and A. L. Fetter, Phys. Rev. B **53**, 5795 (1996).
- <sup>9</sup> I. Affleck, M. Franz, and M. H. S. Amin, Phys. Rev. B **55**, 704 (1997).
- <sup>10</sup> Y. Ren, J. H. Xu, and C. S. Ting, Phys. Rev. Lett. **74**, 3680 (1995).  
J. H. Xu, Y. Ren, and C. S. Ting, Phys. Rev. B **53**, 2991 (1996).
- <sup>11</sup> J. H. Xu, Y. Ren, and C. S. Ting, Phys. Rev. B **52**, 7663 (1995).
- <sup>12</sup> Y. Ren, J. Xu, and C. S. Ting, Phys. Rev. B **53**, 2249 (1996).
- <sup>13</sup> P. I. Soininen, C. Kallin, and A. J. Berlinsky, Phys. Rev. B **50**, 13883 (1994).
- <sup>14</sup> M. Ichioka, N. Enomoto, N. Hayashi, and K. Machida, Phys. Rev. B **53**, 2233 (1996).
- <sup>15</sup> M. Matsumoto and H. Shiba, J. Phys. Soc. Jpn. **64** (1995) 3384, 4867; **65**, 2194 (1996).
- <sup>16</sup> Y. Wang and A. H. MacDonald, Phys. Rev. B **52**, 3876 (1995).
- <sup>17</sup> A. A. Abrikosov, Zh. Eksp. Teor. Fiz. **32**, 1442 (1957) [Sov. Phys. JETP **5**, 1174 (1957)].  
W. H. Kleiner, L. M. Roth, and S. H. Autler, Phys. Rev. **133**, A1266 (1964).
- <sup>18</sup> M. Ichioka, N. Hayashi, N. Enomoto, and K. Machida, Phys. Rev. B **53**, 15316 (1996).
- <sup>19</sup> N. Enomoto, M. Ichioka, and K. Machida, J. Phys. Soc. Jpn. **66**, 204 (1997).
- <sup>20</sup> D. J. Feder and C. Kallin, Phys. Rev. B **55**, 559 (1997).
- <sup>21</sup> G. Eilenberger, Phys. Rev. **164**, 628 (1967).
- <sup>22</sup> K. Takanaka, Prog. Theor. Phys. **46**, 1301 (1971).  
K. Takanaka and T. Nagashima, Prog. Theor. Phys. **43**, 18 (1970).
- <sup>23</sup> H. Won and K. Maki, Phys. Rev. B **53**, 5927 (1996).
- <sup>24</sup> H. Won and K. Maki, Europhys. Lett. **30**, 421 (1995).  
K. Maki, N. Schopohl, and H. Won, Physica B **204**, 214 (1995).  
H. Won and K. Maki, Physica B **199-200**, 353 (1994).
- <sup>25</sup> M. Ichioka, N. Hayashi, and K. Machida, Phys. Rev. B **55**, 6565 (1997).
- <sup>26</sup> See, for example, A. L. Fetter and P. C. Hohenberg, in *Superconductivity*, edited by R. D. Parks (Marcel Dekker, New York, 1969).
- <sup>27</sup> T. Hanaguri, T. Fukase, Y. Koike, I. Tanaka, and H. Kojima, Physica B **165&166**, 1449 (1990).
- <sup>28</sup> Y. Koike, T. Takabayashi, T. Noji, T. Nishizaki, and N. Kobayashi, Phys. Rev. B **54**, 776 (1996).
- <sup>29</sup> T. Ishida, K. Inoue, K. Okuda, H. Asaoka, Y. Kazumata, K. Noda, and H. Takei, Physica C **263**, 260 (1996).  
T. Ishida, K. Okuda, H. Asaoka, Y. Kazumata, K. Noda, and H. Takei, Czechoslovak J. Phys. **46** Suppl. S3, 1217 (1996).
- <sup>30</sup> K. Takanaka and K. Kuboya, Phys. Rev. Lett. **75** (1995) 324.
- <sup>31</sup> K. Takanaka, J. Phys. Soc. Jpn. **65**, 3396 (1997).
- <sup>32</sup> T. Sugiyama and M. Ichioka, in preparation.
- <sup>33</sup> Y. De Wilde, M. Iavarone, U. Welp, V. Metlushko, A. E. Koshelev, I. Aranson, G. W. Crabtree, and P. C. Canfield, preprint.
- <sup>34</sup> M. R. Eskildsen, P. L. Gammel, B. P. Barber, U. Yaron, A. P. Ramirez, D. A. Huse, D. J. Bishop, C. Bolle, C. M. Lieber, S. Oxx, S. Sridhar, N. H. Andersen, K. Mortensen, and P. C. Canfield, Phys. Rev. Lett. **78**, 1968 (1997).

FIG. 1. The configuration of the vortex lattice and the coordinate system. The vortex centers are shown by solid circle. And  $\mathbf{r}_1$  and  $\mathbf{r}_2$  are unit vectors. We set the  $x$  axis along the direction of  $\mathbf{r}_1$ . The  $a$  axis (or the  $b$  axis) forms an angle of  $\theta_0$  from the  $x$  axis (or the  $y$  axis).

FIG. 2. Spatial variation of the induced  $s$ -wave order parameter for the case of a square lattice ( $a_y/a_x = 0.5$ ,  $\zeta = 0.5$ ). (a) Contour plot of the amplitude,  $|s(\mathbf{r})/\gamma s_2^{(1)}|$ . The region  $1.9a_x \times 1.9a_x$  is presented. The  $a$  axis and the  $b$  axis are along the horizontal and the vertical directions. (b) The corresponding position for the vortex of the  $s$ -wave order parameter and its winding number are schematically presented. The solid circle shows the vortex center of the dominant  $d_{x^2-y^2}$ -wave order parameter, where the induced  $s$ -wave component has a vortex with winding number  $-1$ . The  $s$ -wave component has an extra vortex at the point marked  $x$ . The solid line shows the unit cell of the vortex lattice.

FIG. 3. The same as Fig. 2, but for the case of an oblique lattice ( $a_y/a_x = 0.676$ ,  $\zeta = 0.5$ ).

FIG. 4. The equilibrium state of the vortex lattice is schematically presented for the case (a). Vortices form a shape of an isosceles triangle with  $OA = AB$ , where the base  $OA$  is along the  $a$  axis.

FIG. 5. Temperature dependence of the unit cell shape of the vortex lattice. The ratio  $a_y/a_x$  along the curve of  $H_{c2}(T)$  is presented as a function of  $T/T_c$  for various mixing of the  $s$ -wave component,  $c_s = -0.2, -0.1, 0, 0.2, 0.4$ . A thick line shows the pure  $d_{x^2-y^2}$ -wave case ( $c_s = 0$ ). The angle  $B$  in Fig. 4 gradually varies from  $60^\circ$  ( $a_y/a_x = 0.866$ ) to  $90^\circ$  ( $a_y/a_x = 0.5$ ), when temperature is lowered from  $T_c$ .

FIG. 6. Spatial variation of the  $d_{x^2-y^2}$ -wave order parameter. Contour plot of the amplitude,  $|d(\mathbf{r})/d_0|$ , is presented. (a) The case of a square lattice ( $a_y/a_x = 0.5$ ,  $\zeta = 0.5$ ) with an equilibrium orientation  $\theta_0 = 0^\circ$  for  $\gamma = 0.2$ . (b) The case of a square lattice with an unstable orientation  $\theta_0 = 45^\circ$  for  $\gamma = 0.2$ . (c) The case of an oblique lattice ( $a_y/a_x = 0.676$ ,  $\zeta = 0.5$ ) with an equilibrium orientation  $\theta_0 = 0^\circ$  for  $\gamma = 0.115$ . The region  $1.9a_x \times 1.9a_x$  is presented, where one of the vortex centers locates at the center of the figure. The  $a$  axis and the  $b$  axis are along the horizontal and the vertical directions.

FIG. 7. Spatial variation of the current. Contour plot of the amplitude,  $|\mathbf{j}(\mathbf{r})|/(\pi\epsilon^{1/2}\xi/2\kappa^2\eta^2)$ , is presented. (a), (b) and (c) correspond to the cases of Fig. 6 (a), (b) and (c), respectively.

FIG. 8. Spatial variation of the induced magnetic field. The contour plot of  $h_z(\mathbf{r})/|h_z^{(0)}|$  is presented. (a), (b) and (c) correspond to the cases of Fig. 6 (a), (b) and (c), respectively.

FIG. 9. The magnetic field distribution function  $P(h)$  as a function of  $h/|h_z^{(0)}|$  for various temperatures;  $\gamma = 0$  (a), 0.06 (b), 0.115 (c), 0.15 (d) and 0.2 (e), which correspond to  $T/T_c = 1, 0.936, 0.881, 0.848$  and  $0.802$ , respectively. Solid lines are for the case of a  $d_{x^2-y^2}$ -wave superconductor, where (a) is the triangular lattice, (b) and (c) the oblique lattice, (d) and (e) the square lattice. There, parameters are set as  $\zeta = 0.5$ ,  $\theta_0 = 0$  and  $a_y/a_x = 0.866$  (a), 0.799 (b), 0.676 (c), 0.5 (d), 0.5 (e). Dotted lines are for the case of an isotropic  $s$ -wave superconductor, where (a)-(e) are the triangular lattice ( $\zeta = 0.5$ ,  $a_y/a_x = 0.866$ ). For clarity, the curves have been sifted along the vertical axis.

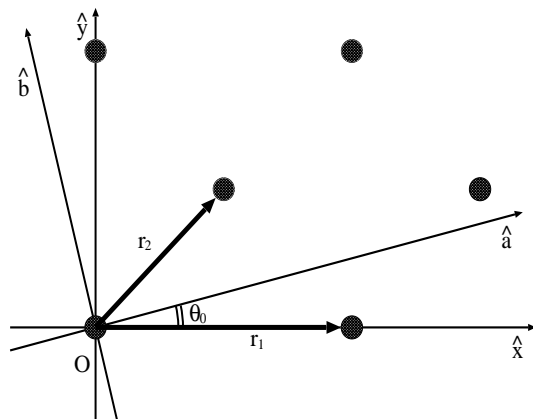


Fig. 1

This figure "ichiokaFig2.gif" is available in "gif" format from:

<http://arxiv.org/ps/cond-mat/9704147v1>

This figure "ichiokaFig3.gif" is available in "gif" format from:

<http://arxiv.org/ps/cond-mat/9704147v1>

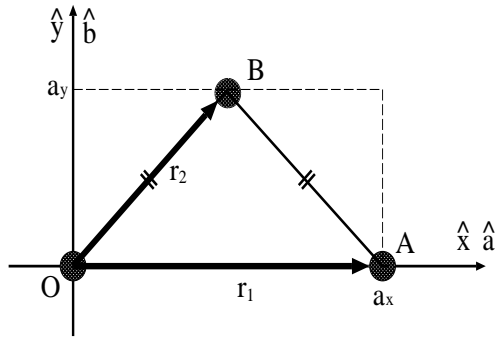


Fig. 4

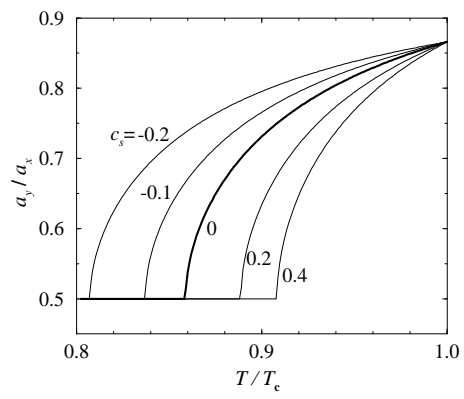


Fig. 5



This figure "ichiokaFig6.gif" is available in "gif" format from:

<http://arxiv.org/ps/cond-mat/9704147v1>

This figure "ichiokaFig7.gif" is available in "gif" format from:

<http://arxiv.org/ps/cond-mat/9704147v1>

This figure "ichiokaFig8.gif" is available in "gif" format from:

<http://arxiv.org/ps/cond-mat/9704147v1>

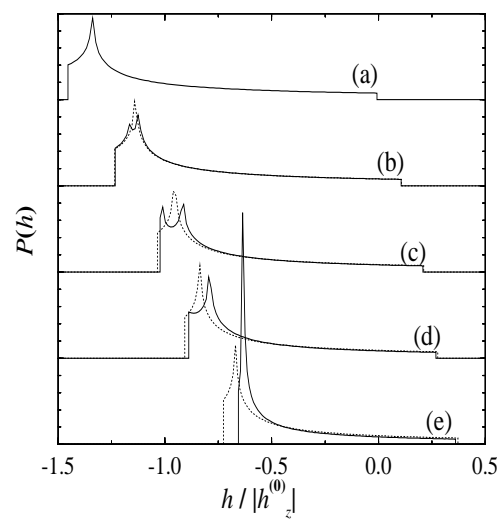


Fig. 9